



TECHNICAL REPORT
NATICK/TR-92/012

AD A 251 384

AN IMPROVED SCALING LAW FOR DETERMINING STIFFNESS OF FLAT, CIRCULAR CANOPIES

Eugene E. Niemi, Jr.

University of Lowell
Lowell, MA 01854

MARCH 1992

Final Report
December 1988 - December 1989

APPROVED FOR PUBLIC RELEASE;
DISTRIBUTION UNLIMITED

Prepared for
UNITED STATES ARMY NATICK
RESEARCH, DEVELOPMENT AND ENGINEERING CENTER
NATICK, MASSACHUSETTS 01760-5000

AERO-MECHANICAL ENGINEERING DIRECTORATE

U. S. ARMY NATICK RD&E CENTER
ATTN: STRNG-MIL
NATICK, MA 01760-5040

DISCLAIMERS

The findings contained in this report are not to be construed as an official Department of the Army position unless so designated by other authorized documents.

Citation of trade names in this report does not constitute an official endorsement or approval of the use of such items.

DESTRUCTION NOTICE

For Classified Documents:

Follow the procedures in DoD 5200.22-M, Industrial Security Manual, Section II-19 or DoD 5200.1-R, Information Security Program Regulation, Chapter IX.

For Unclassified/Limited Distribution Documents:

Destroy by any method that prevents disclosure of contents or reconstruction of the document.

REPORT DOCUMENTATION PAGE

Form Approved
OMB No. 0704-0188

Public reporting burden for this collection of information is estimated to average 1 hour per response, including the time for reviewing instructions, searching existing data sources, gathering and maintaining the data needed, and completing and reviewing the collection of information. Send comments regarding this burden estimate or any other aspect of this collection of information, including suggestions for reducing this burden, to Washington Headquarters Services, Directorate for Information Operations and Reports, 1215 Jefferson Davis Highway, Suite 1204, Arlington, VA 22202-4302, and to the Office of Management and Budget, Paperwork Reduction Project (0704-0188), Washington, DC 20503.

1. AGENCY USE ONLY (Leave blank)		2. REPORT DATE March 1992	3. REPORT TYPE AND DATES COVERED FINAL December 1988 - December 1989	
4. TITLE AND SUBTITLE AN IMPROVED SCALING LAW FOR DETERMINING STIFFNESS OF FLAT, CIRCULAR CANOPIES			5. FUNDING NUMBERS IPA 05-5179 AGG CODE: T/B 1344	
6. AUTHOR(S) Eugene E. Niemi, Jr.				
7. PERFORMING ORGANIZATION NAME(S) AND ADDRESS(ES) University of Lowell One University Ave. Lowell, MA 01854			8. PERFORMING ORGANIZATION REPORT NUMBER	
9. SPONSORING/MONITORING AGENCY NAME(S) AND ADDRESS(ES) U.S. Army Natick RD&E Center ATTN: STRNC-UE Natick, MA 01760-5017			10. SPONSORING/MONITORING AGENCY REPORT NUMBER NATICK/TR-92/012	
11. SUPPLEMENTARY NOTES				
12a. DISTRIBUTION AVAILABILITY STATEMENT Approved for public release; distribution unlimited			12b. DISTRIBUTION CODE	
13. ABSTRACT (Maximum 200 words) The scaling of parachute canopy fabric stiffness is important if wind tunnel model or drop test data are to be used to predict full-scale parachute performance. The use of scale models in development testing is desirable because they can save significant cost and time in the development cycle. Theories for parachute opening dynamics, dimensional analyses and test data were reviewed to determine the effects of parachute canopy scale and stiffness on the opening characteristics. Based on this work, a new relative stiffness index for parachute canopies has been developed. This index gives good data correlation for parachute opening time for solid flat circular canopies over a wide range of canopy diameters and fabric areal densities. This relative stiffness index will make it possible to use scale model wind tunnel and drop test data with more confidence than in the past.				
14. SUBJECT TERMS PARACHUTE OPENING TIME FABRIC STRENGTH PARACHUTE CANOPIES PARACHUTE OPENING DYNAMICS SCALE MODELS FLAT PLATE CANOPIES FLEXURAL STRENGTH SCALING PARACHUTE OPENING STIFFNESS FLEXURAL RIGIDITY			15. NUMBER OF PAGES 67	
			16. PRICE CODE	
17. SECURITY CLASSIFICATION OF REPORT UNCLASSIFIED	18. SECURITY CLASSIFICATION OF THIS PAGE UNCLASSIFIED	19. SECURITY CLASSIFICATION OF ABSTRACT UNCLASSIFIED	20. LIMITATION OF ABSTRACT	

Table of Contents

List of Illustrations	v
List of Tables	vi
List of Symbols	vii
Preface	xi
INTRODUCTION	1
REVIEW OF DIMENSIONAL ANALYSES AND SCALING PARAMETERS	2
REVIEW OF OPENING DYNAMICS THEORIES	8
Effect of Canopy Stiffness on Opening Dynamics	12
Two Extremes of Stiffness Effects	14
DEVELOPMENT OF RELATIVE STIFFNESS INDEX	15
Modification of Form for Relative Stiffness Index	17
Physical Significance of Relative Stiffness Index	19
Overview	20
EVALUATION OF FABRIC PROPERTIES	21
Biaxial Test Data	21
Uniaxial Fabric Test Data	24
Linear, Orthotropic Fabric Model	25
APPLICATION OF METHOD TO EXPERIMENTAL DATA	
CORRELATION	28
C-9 Parachute Test Data	28
Opening Time Data Correlation, Mass Ratio 0.13	29
Opening Time Data Correlation, Mass Ratio 0.20	29
Wind Tunnel Data	34
Application of the Method to 35 ft Do T-10 Parachutes	35
Large Diameter Parachutes (G-12 and G-11)	41

OPENING SHOCK CORRELATION PARAMETERS	42
Correlation Study for Opening Shock	40
Effect of Suspension Line Elasticity	43
Modified Impulse Concept	43
Use of Modified Impulse Parameter	46
 CLOSURE	 48
Recommendations for Future Research	48
Use of Theories to Predict Canopy Stiffness Effects	48
Additional Verification of Relative Stiffness Index and Modified Impulse	49
Relative Stiffness for Other Canopy Designs	49
Conclusion	50
 REFERENCES	 51



Accession For	
NTIS GRA&I	<input checked="" type="checkbox"/>
DTIC TAB	<input type="checkbox"/>
Unannounced	<input type="checkbox"/>
Justification	
By _____	
Distribution/	
Availability Codes	
Dist	Special
A-1	

List of Illustrations

<u>Figure</u>		<u>Page</u>
1	Geometric model of parachute canopy at the start of filling	6
2	Calculated non-dimensional filling time, τ_f , as a function of mass ratio, μ_T , for various Froude numbers. C-9 parachute in vertical drops	10
3	Opening shock force F_f (non-dimensionalized) as a function of Froude number F_T and mass ratio μ_T . C-9 parachute in vertical drops	11
4	Effect of mass ratio on peak load factor for C-9 parachute deployed at various Froude numbers	13
5	Biaxial stress-strain relationships for 50 g/m ² plain weave British nylon parachute fabric	23
6	Opening time as a function of Froude number for full-scale and 1/4-scale C-9 parachutes at mass ratio 0.13	30
7	Opening time as a function of relative stiffness index for full-scale and 1/4-scale C-9 parachutes at mass ratio 0.13	31
8	Opening time as a function of relative stiffness index for full-scale, 1/2-scale, and 1/4-scale C-9 parachutes at mass ratios 0.13 and 0.20	32
9	Opening time as a function of Froude number for full-scale, 1/2-scale, and 1/4-scale C-9 parachutes at mass ratios 0.13 and 0.20	33
10	Non-dimensional filling time as a function of relative stiffness index for T-10 and other parachute configurations	36
11	Filling time vs. snatch velocity for T-10 extended skirt canopy and high strength canopy	37
12	Non-dimensional filling time vs. Froude number for T-10 extended skirt canopy and high strength canopy	38
13	Non-dimensional filling time vs. Froude number of operation for T-10 extended skirt canopy and high strength canopy	39
14	Non-dimensional opening shock and non-dimensional opening time for three C-9 type parachutes, mass ratio 0.13	44
15	Modified impulse vs. Froude number for C-9 type parachutes of various configurations and mass ratios	47

List of Tables

<u>Table</u>		<u>Page</u>
1	Properties of 1.47 oz/yd ² plain weave, British nylon parachute fabric	22
2	Values of Poisson's ratio for MIL-C-7020-1 type parachute fabric using Eqs. (13) and (14)	26
3	Uniaxial test data for Young's Modulus and average values used for analysis	27
4	Range of test variables covered in Lee's tests	28

List of Tables

Table		Page
1	Properties of 1.47 oz/yd ² plain weave, British nylon parachute fabric	22
2	Values of Poisson's ratio for MIL-C-7020-1 type parachute fabric using Eqs. (13) and (14)	26
3	Uniaxial test data for Young's Modulus and average values used for analysis	27
4	Range of test variables covered in Lee's tests	28

List of Symbols

<u>Symbol</u>	<u>Explanation</u>
a	speed of sound (also c_s)
c	air permeability
C_D	drag coefficient
c_{eff}	effective porosity of canopy fabric
c_f	shroudline spring constant (also k)
c_s	speed of sound (also a)
D	parachute diameter (projected)
d	diameter of fabric threads, or initial open mouth diameter of canopy, or spring constant of suspension lines
D_0	parachute constructed diameter
D_z	damping factor
E	Young's modulus of canopy material
e_c	canopy rigidity
e_s	shroudline elasticity
F	force
f	dimensionless force
f_1, f_2	functional relationship symbols
Fr	Froude number
F_z	elastic factor
g	acceleration due to gravity
h	lateral length of truncated cone of opening canopy
I	canopy inertia number, or second moment of area of fabric cross-section

List of Symbols (Continued)

<u>Symbol</u>	<u>Explanation</u>
k	shroudline spring constant
K_p	parachute spring constant
k_s	shroudline spring constant
l	characteristic length, or length of suspension line under load
M	Mach number
m	mass (of canopy, payload, or system, as defined)
M_r	mass ratio (used with subscript)
m_s	suspended (payload) mass
n	number of suspension lines
R	Reynolds number
R_e	Reynolds number
R_f	Reynolds number of fabric
R_m	added air mass
S	projected area of canopy at any instant of time
s	distance between the center of mass of payload and parachute
S_{mn}	coefficients in stress-strain equations
S_0	projected area of constructed canopy diameter
T	total filling time
t	time, or thickness of fabric
V	velocity
v	velocity
w	areal density (canopy or canopy fabric)

List of Symbols (Continued)

<u>Symbol</u>	<u>Explanation</u>
β_0	initial semi-aperture angle of suspension lines
ϵ	strain in fabric
γ	trajectory inclination angle (same as γ_0)
η	parachute stiffness index
ρ	air density
σ	stress in fabric
τ	non-dimensional opening time
τ_f	non-dimensional filling time
ν	kinematic viscosity of air, or Poisson's ratio of fabric
Ω	stiffness
W_c	weight of canopy (same as W_p)
W_p	weight of parachute (same as W_c)
X	non-dimensional opening shock (g's)
ζ	relative stiffness index of parachute canopy
μ	dynamic viscosity of air
μ_T	mass ratio (total, for canopy and payload)

Subscripts

ave	average
c	canopy
cl	cloth (or parachute fabric)

List of Symbols (Concluded)

Subscripts

f	filling, fabric, or fill direction
i	initial
L	payload, or suspended load
l	load
max	maximum
min	minimum
o	initial, or constructed
p	peak value, or parachute
s	snatch, or suspended
T	total
w	warp direction
1, 2	referring to two orthogonal directions

Superscripts

'	modified value
''	modified value
—	average

Preface

This report was prepared by the University of Lowell as part of IPA Research Project No. 05-5179. The work described in this report was performed between December 15, 1988, and December 14, 1989.

The work accomplished under this contract was sponsored by the U.S. Army Natick Research, Development and Engineering Center, Aero-Mechanical Engineering Directorate, Engineering Technology Division. Dr. Earl C. Steeves was the project supervisor.

AN IMPROVED SCALING LAW FOR DETERMINING STIFFNESS FOR FLAT, CIRCULAR CANOPIES

INTRODUCTION

In the design and development of parachutes, it is often convenient to rely on scale models for drop testing or wind tunnel testing. The use of scale models in development testing can save significant cost and time in the development cycle. Because the parachute scaling laws are not completely understood, the interpretation of model test data poses numerous problems. For example, model parachutes tend to open quicker, with a larger scaled opening shock force, than their full-scale counterparts.

For the scaling of parachutes, there are several unsettled questions concerning the scaling of the fabric stiffness. Scale models of parachutes have customarily been made from the same weight fabric as the prototype. This makes the scale model canopy relatively stiff compared to full-scale. Heinrich recognized this and developed a stiffness index to compare model and prototype and did research on canopy construction techniques needed to make the model fabric stiffness more nearly that of the prototype. However, even using modified construction techniques, it has not been possible to find ways to make the models quite as flexible as the prototype.

This report presents an investigation of the parachute scaling laws applicable to the opening process. The object was to find a better correlation parameter for opening time so models can still be stiffer than the prototypes, but that model test conditions can be altered to make the model data more usable to predict full-scale performance. To accomplish this, existing theories for parachute opening dynamics were reviewed, existing test data were analyzed, and parachute canopy fabric properties were examined. No new theories were developed and no new experiments were conducted as part of this study. The end result of this study was the identification of a better correlation parameter for opening time than any currently available to predict prototype parachute performance.

REVIEW OF DIMENSIONAL ANALYSES AND SCALING PARAMETERS

Over the years, a number of dimensional analyses of the parachute filling process have been conducted. These analyses have identified the importance of the Froude number (ratio of inertia to gravity forces) and mass ratio on parachute opening time and shock. Other parameters identified as being of somewhat lesser importance are the Reynolds number, fabric porosity, shroudline elasticity and damping, canopy stiffness, and canopy mass ratio (or inertia number).

The more important of these investigations have been conducted by Kaplun [1], Barton [2], French [3,4], Fu [5], and Lingard [6]. Only a summary of the major results will be presented here.

One of the first investigators to point out the importance of parachute elastic properties was Kaplun [1]. Quoting from his work:

The specification of the *elastic properties* of the parachute is so complicated that, at least, some departures from rigor will be unavoidable. Properly, considering the fabric to be a plastic, anisotropic medium, it would be necessary to specify twenty-one elastic parameters, and, in addition to the similarity of distribution, require that the stress-strain diagrams remain similar. Let us tentatively take the other extreme by assuming that the *spring constant of the shroudlines* and the *flexural rigidity of the canopy* are the only important factors. Whether this assumption is actually justified can be decided only on the basis of consistency of the experimental data derived from it. However, it should be mentioned that rigidity, which varies inversely as the fourth power of the diameter, is especially important in small models.

Kaplun considered the case of a parachute attached to a fixed support, thus the Froude number did not appear in the results of his evaluation. He came up with a set of six dimensionless parameters, choosing the combinations of parameters based on expected physical significance. The list of parameters selected was the following:

$$\text{Reynolds number} \quad R = \frac{VD\rho}{\mu}$$

$$\text{Reynolds number of the fabric} \quad R_f = \frac{Vd\rho}{\mu}$$

$$\text{Mach number} \quad M = \frac{V}{a}$$

$$\text{Shroudline elasticity} \quad e_s = \frac{k}{\rho V^2 D}$$

Canopy rigidity

$$e_c = \frac{(EI)}{\rho V^2 D^4}$$

Canopy inertia number

$$I = \frac{m}{\rho D^3}$$

Based on these independent parameters, the dimensionless dependent parameters were selected as dimensionless time,

$$\tau = \frac{Vt}{D}$$

where total filling time T is given by

$$\frac{VT}{D} = f_1 (R, R_f, M, e_s, e_c, I)$$

and dimensionless force

$$f = \frac{F}{\frac{1}{2} \rho V^2 \left(\frac{\pi D^2}{4} \right)}$$

where maximum opening force, F_{max} , is given by

$$\frac{F_{max}}{\frac{1}{2} \rho V^2 D^2} = f_2 (R, R_f, M, e_s, e_c, I)$$

Although Kaplun did not use Froude number as one of his variables, he defined it as follows:

$$Fr = \frac{\frac{1}{2} \rho V^2 D^2}{m_s g}$$

Using *this* definition with the case of a parachute tied to a fixed support (infinite mass inflation) gives a Froude number of zero. Other investigators define Froude number differently, as pointed out later.

Kaplun pointed out that, if it is assumed that these parameters have *no* effect, then the expressions for the performance variables would only be determined up to a constant of proportionality, i.e.,

$$\frac{VT}{D} = \text{constant}$$

and

$$\frac{F_{\max}}{\frac{1}{2}\rho V^2 D^2} = \text{constant}$$

For certain ranges of operation, this type of behavior has been observed for the non-dimensional filling time, as noted later.

It should be noted that Kaplun did not define how the "flexural rigidity," EI , of a parachute canopy should be interpreted or determined, either analytically or experimentally. The canopy flexural rigidity must be evaluated in some manner that is physically consistent with its effect on parachute opening dynamics. Heinrich [7] did work in this area and defined a "canopy stiffness index" quite different from Kaplun's canopy rigidity parameter. However, Heinrich's index is useful only for comparing canopies or in attempting to construct scale model canopies with the same flexibility as a prototype canopy. But it does not let someone use data on a stiff canopy model to predict the performance of a more flexible prototype. This determination is one of the contributions of the current study.

Fu [5] developed a theory to predict parachute opening behavior, and reviewed dimensional analyses conducted by previous investigators. In addition to scaling geometric parameters between model and prototype, Fu identified the following parameters as needing consideration:

$$\text{Froude number, } Fr = \frac{V_s^2}{gD_0}$$

$$\text{Mass ratio, } \mu_T = \frac{m_T}{\rho D_0^3}$$

Initial trajectory angle, γ_0

$$\text{Elastic factor, } F_z = \frac{nc_f D_o^2}{m_L V_s^2}$$

$$\text{Damping factor, } D_z = \frac{nd D_o}{m_L V_s}$$

Effective porosity, C_{eff}

Payload to system mass ratio, $\frac{m_L}{m_T}$

The effect of canopy stiffness was not considered directly by Fu, but some of its implicit effects were accounted for as an initial input to the theory, in the form of semiapertural angle, β_0 (see Fig. 1). This angle determines the initial parachute mouth area available for air capture. Empirical values for β_0 were obtained by Fu from films of parachute opening, and the value of β_0 would certainly be affected in part by canopy stiffness.

In [8], the important dimensionless correlation parameters are summarized as follows:

Name	Parameter	Symbol	Factor
Reynolds No.	$lv\rho/\mu$	Re	Scale
Mach No.	v/c_s	M	Compressibility
Froude No.	$v/(lg)^{1/2}$	Fr	Fluid displacement
Kaplun No.	$\kappa/\rho v^2 l$	Kp	Stretching resistance (1/elasticity)
Relative stiffness	$EI/\rho v^2 l^4$	Ω	Stiffness (1/flexibility)
Mass Ratio	$\rho l^3/m$	Rm	Added air mass
Effective Porosity	v_λ/v^*	C_{eff}	Air permeability

Here again, the relative stiffness parameter, $\Omega = \frac{EI}{\rho v^2 l^4}$, is presented without any indication of how to evaluate the canopy "flexural rigidity," EI.

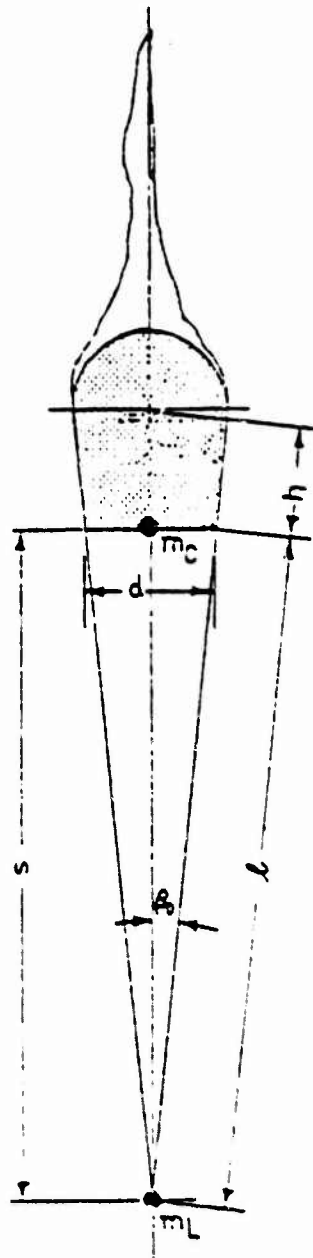


Fig. 1: Geometric model of parachute canopy at the start of filling.
(Figure taken from Ref. 5)

In [9], Lee shows that time to peak opening shock, τ , and the value of peak opening shock, X_p , are functions of mass ratio, Froude number, canopy stiffness index, and parachute spring constant:

$$X_p, \tau = f(M_r, Fr, \eta, K_p)$$

where canopy stiffness index $\eta = \left(\frac{D_{max}}{D_o}\right) \left(\frac{W_c}{S_o W_{cl}}\right)$, parachute spring constant $K_p = \frac{k_s D_o}{m_1 g}$.

It was shown that matching of M_r and Fr and satisfying geometric similarity would not necessarily guarantee scaling τ and X_p because other parachute properties had to be considered also; these include fabric mass density and porosity, canopy flexibility, and suspension line stiffness.

Steeves [10] showed from dimensional analysis that the scaling of a parachute opening requires that the canopy fabric areal density ratio between model and full-scale be the same as the geometric dimensional ratio and that the fabric porosity ratio be the square root of the geometric ratio.

Lee concludes that "...the present moderate amount of data show that X_p and τ of full-scale parachutes at a given Fr and M_r can be reasonably well predicted from the measurement of X_p and τ of small-scale models with similar η and K_p as those of the full scale."

One of the difficulties in satisfying the above requirements is to be able to build small-scale models with sufficiently low stiffness indices, η , to match the prototype parachute stiffness. A way to avoid the requirement for matching η would be to develop a "relative" or "effective" stiffness index that would allow scaling data from stiffer models to more flexible prototypes by use of a suitably modified scaling parameter.

REVIEW OF OPENING DYNAMICS THEORIES

It was not the purpose of this study to develop any new theories for parachute opening dynamics, but rather to use test data together with dimensional analysis techniques to develop correlation parameters that would include the effects of parachute canopy stiffness. However, to aid in interpreting the test data, and to guide in the development of correlation parameters, some theories were examined.

A listing of some of the early opening dynamics theories can be found in [11-20]. Many of these methods require difficult to measure empirical inputs, such as the change in projected canopy area with time. The two theories that proved most useful for the current study were those developed by Fu [5] and Lingard [6]. The dimensional analysis work conducted by Fu was summarized earlier in this report.

Fu develops a theory to predict parachute opening shock and time, using a minimum of experimental inputs based on as little test data as possible. Fu considers the payload and canopy as two point masses connected by spring with damping. The canopy shape is represented as a truncated cone topped with a hemispherical cap. The apparent mass of the parachute is assumed to be proportional to the canopy volume. The canopy vent size and effective porosity of the canopy fabric are considered in the conservation of mass equations used to model canopy filling. Using Newton's law, conservation of mass, and the appropriate geometric relations, a system of non-linear differential equations was solved numerically.

Fu studied the effect of the following variables on opening time and opening shock:

- a. Froude number
- b. mass ratio
- c. deployment flight path angle
- d. suspension line elasticity and damping
- e. suspension line semi-aperture angle at the beginning of inflation

All of Fu's comparisons between theory and experiment were for the 28 ft diameter C-9 parachute. For the test data that Fu had available, satisfactory agreement between theory and experiment was obtained. For example, the maximum deviation of the maximum filling force was less than 10% of the measured values. This is certainly satisfactory agreement in parachute technology, since the variations occurring in experiments are usually considerably larger.

Fu's theory provides two important graphs of relevance for the current study. These graphs are shown as Figs. 2 and 3. Fig. 2 is a plot of non-dimensional filling time vs. mass ratio for various Froude numbers for vertical deployments of a C-9 type parachute. Examination of this figure shows that the effect of Froude number variation on non-dimensional opening time is predicted to be quite small, except at very low mass ratios. Non-dimensional opening time *does* vary with mass ratio, but at mass ratio above 0.1, the variation is small. As mass ratio increases from 0.1 to 10.0, the predicted non-dimensional opening time decreases only from six to four.

As shown in Fig. 3, the variation of opening *shock* with both Froude number and mass ratio can be quite large. Based on these graphs, it may be reasonable to look for different correlating parameters for opening time than for opening shock.

Lingard's analysis for predicting opening shock is considerably different from that of Fu, but leads to similar results. His method is intended to provide a relatively simple theory to let a designer perform tradeoffs upon the effects on the peak load of parameters such as snatch velocity, suspended mass, parachute size, and altitude and angle of deployment. The main assumptions made by Lingard are as follows:

- a. The parachute inflates in a constant non-dimensional opening time independent of snatch velocity and mass ratio.
- b. For a given parachute design, there exists a unique force coefficient vs. non-dimensional time function, which is independent of snatch velocity or mass ratio.

These two assumptions are then used to extract empirical data from a small number of full-scale tests of a particular solid cloth parachute system. With these assumptions, Newton's second law is then used to develop a model that allows calculation of force and velocity profiles during deployment, and the effects of the

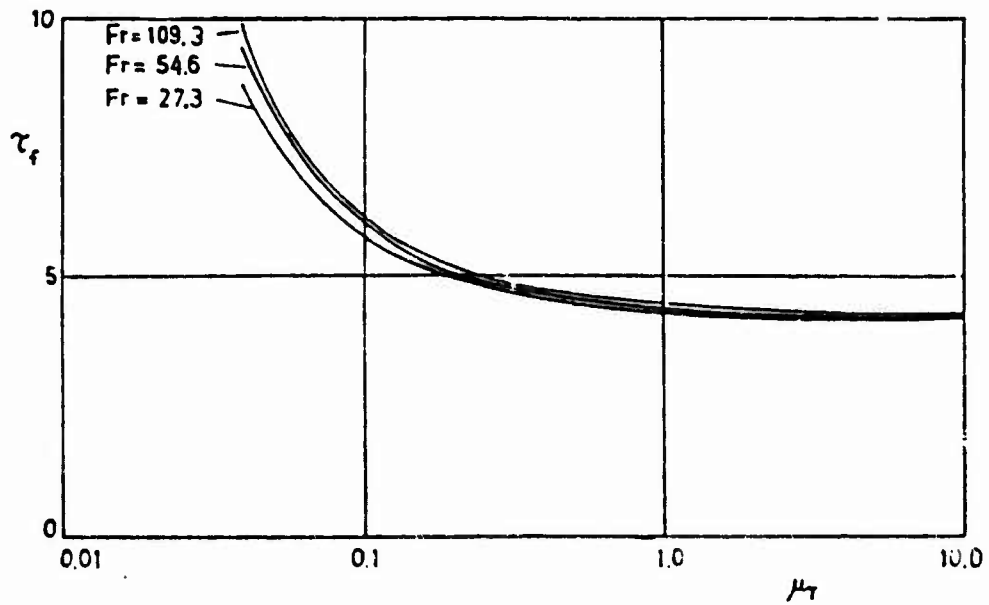


Fig. 2: Calculated non-dimensional filling time, τ_f , as a function of mass ratio, μ_T , for various Froude numbers.
 C-9 parachute in vertical drops.
 (Figure taken from Ref. 5)

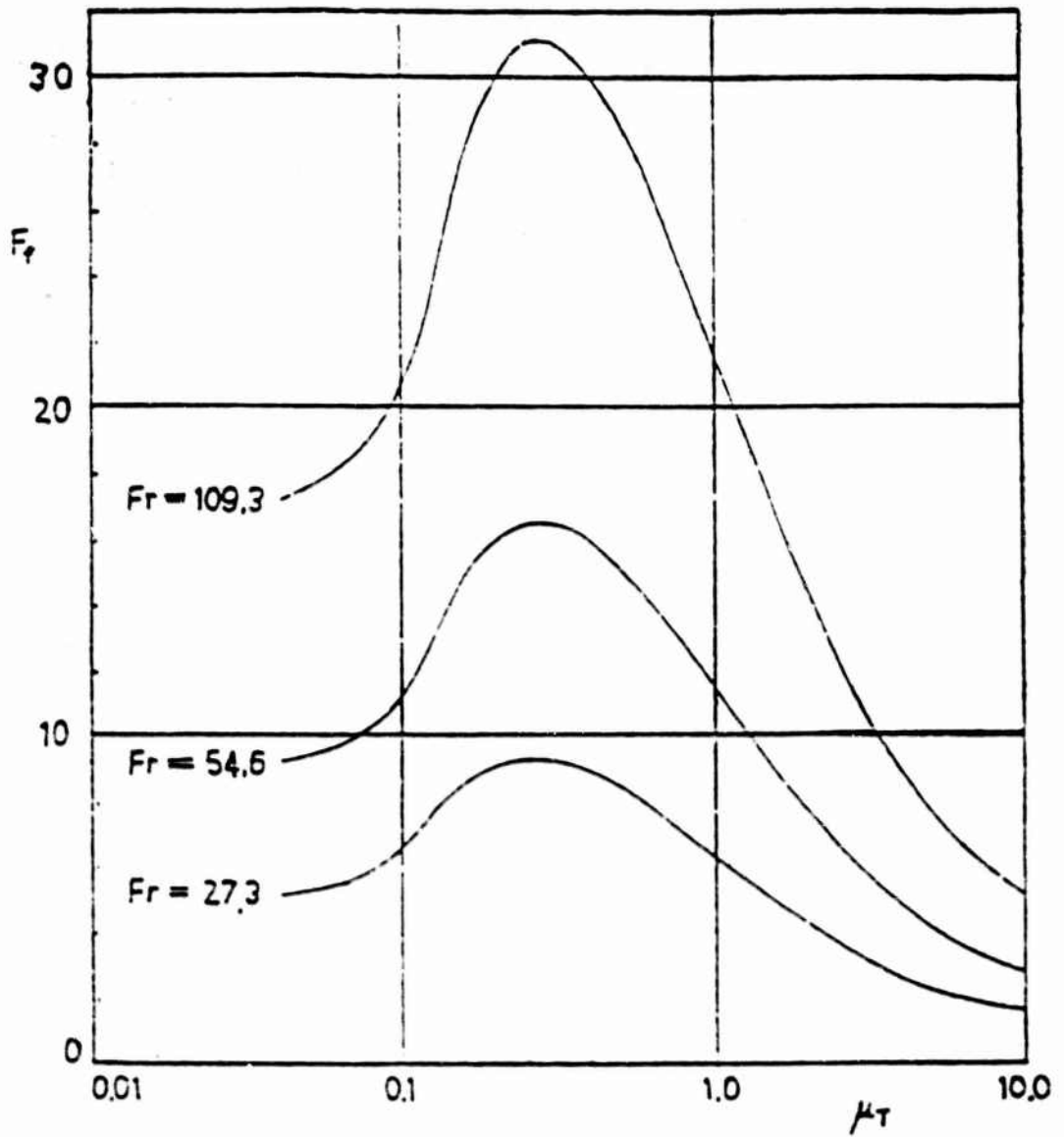


Fig. 3: Opening shock force F_f (non-dimensionalized) as a function of Froude number Fr and mass ratio μ_T .
 C-9 parachute in vertical drops.
 (Figure taken from Ref. 5)

above-mentioned variables on deployment can be studied. Lingard's results for non-dimensional opening shock are shown in Fig. 4.

Comparison of Figs. 3 and 4 shows similar trends from two totally different approaches and lends confidence to the results obtained. Because of assumption (a) used above, Lingard's method is not useful in predicting Froude number and mass ratio effects on opening time, but the assumption itself agrees fairly well with the theoretical results presented from Fu in Fig. 2.

In later evaluations of experimental data in this report, the trends shown in Figs. 2 through 4 will be referred to for guidance in evaluating the importance of various parameters in data correlation.

Effect of Canopy Stiffness on Opening Dynamics

The stiffness of the canopy affects the dynamics of the opening process in at least three ways: at the time of parachute snatch, in the "lines taught" configuration, the canopy stiffness affects the suspension line semi-aperture angle, β_0 , and the amount of open mouth diameter, d , available for the beginning of the filling process (see Fig. 1).

The stiffness subsequently affects the "unfolding process" of the parachute as it goes from the cylindrical streaming configuration to a hemispherical shape. Finally, the stiffness affects the amount of canopy and suspension line stretching, or "overexpansion" that occurs once the canopy has reached the hemispherical shape.

In most parachute opening theories, the only way the *canopy* stiffness can enter the theory is through the initial value of β_0 and d at the time of snatch. Some theories, for example that of Payne [14], do consider suspension line stiffness, but not canopy stiffness. In Lingard's theory, the effect of canopy and suspension line stiffnesses are automatically included in the theory because of the way the characteristic force-time signature is obtained from the test data. However, a characteristic force-time signature obtained for one size canopy-suspension line configuration may not be valid for a different size canopy-suspension line configuration. Thus, Lingard's theory may not work for significant changes in

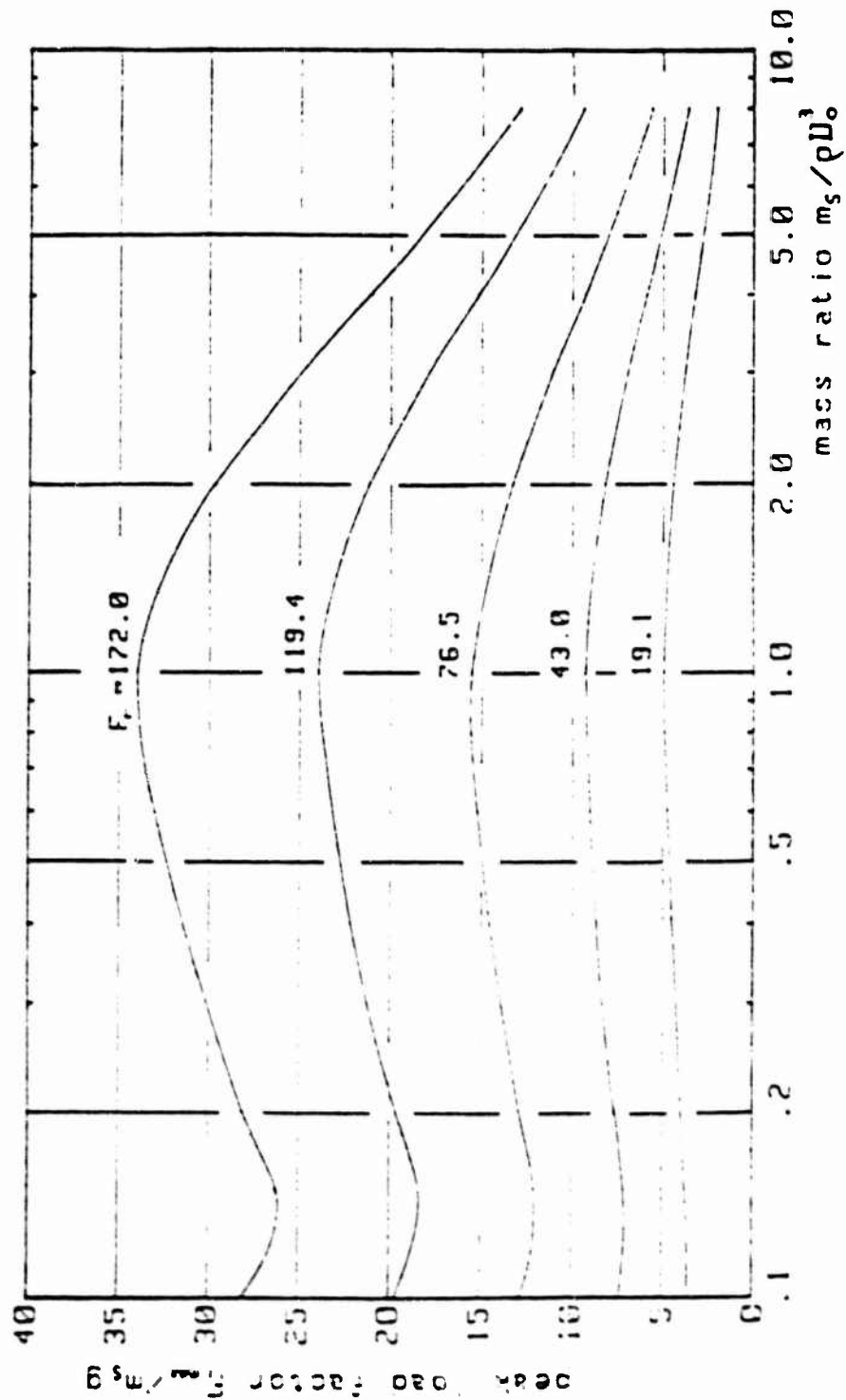


Fig. 4 - Effect of mass ratio on peak load factor for C-9 parachute deployed at various Froude numbers. (Figure taken from Ref. 6)

canopy or suspension line modulus of elasticity, fabric areal density, or fabric porosity. In this case, a theory more like Fu's or Payne's would be needed.

Two Extremes of Stiffness Effects

There are two limiting conditions in which parachute stiffness or flexibility would act in different ways. One extreme would be the case where the parachute is of large diameter and constructed from a thin fabric. In this case, the parachute opening dynamics would be governed mostly by the initial parachute "open mouth" area $(C_D S)_i$, plus the elasticity of the fabric itself as expressed by Young's modulus, E . In this case, the concept of "flexural rigidity" (EI term) as used in beam and plate bending theories would have no significance.

The other extreme would be the case where the parachute is of small diameter and constructed from relatively "thick" fabric. In this case, upside down hang tests would show a large initial parachute "open mouth" diameter, as expressed in Heinrich's original stiffness index formulation. It is expected that the flexural rigidity concepts used in beam and plate theories might be appropriate here in describing opening dynamics. Test data on the fabric crease resistance would be useful here. This extreme is probably best exemplified in very small wind tunnel model tests.

In each case (or at each extreme), the question arises as to which non-dimensional parameters can be used to correlate opening dynamics behavior, and what can be used as a measure of the dividing line for the two kinds of behavior.

DEVELOPMENT OF RELATIVE STIFFNESS INDEX

Up to this point in time, it appears that the only measure of parachute canopy stiffness that has been used extensively is the one developed by Heinrich and discussed earlier in this report in the review of Lee's work [9]. As mentioned earlier, the main value of the Heinrich index is to compare stiffnesses of various canopies and for use as a basis for developing model canopies that might approach prototype canopy stiffness. The Heinrich index does not allow one to take data from a stiffer model canopy and use it to predict the behavior of a more flexible prototype, or vice versa. In this section, a new "relative stiffness index" is proposed that allows one to perform these data correlations, especially for parachute opening time.

After considering available test data and opening theories and reviewing the dimensional analyses conducted to date, the author concludes the main parameter that would appear to affect stiffness differences between model and full scale is the "canopy rigidity" or "relative stiffness" term proposed by Kaplun in the form

$$e_c = \frac{(EI)}{\rho V^2 D^4}$$

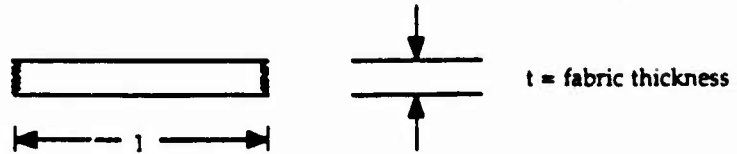
or in [8] as

$$\Omega = \frac{EI}{\rho V^2 l^4} = \frac{EI}{\rho V^2 D^4}$$

In neither reference is any information given on methods for evaluating canopy second moment of area, I .

The approach used to develop this concept in the present work was as follows:

The numerator is actually an expression for the flexural rigidity term used in beam bending theory. If a unit width of parachute fabric is considered as a "beam," the second moment of area would be evaluated as shown in the figure below:



$$I = \frac{(1)t^3}{12}$$

Beam theory, of course, does not apply unless $t > \text{width}$. Since the second moment of area I (commonly called moment of inertia), dimensionally must have units of length to the fourth power, the expression for Ω was modified by writing it in the form

$$\Omega = \frac{E \left[\frac{Dt^3}{12} \right]}{\rho V^2 D^4} = \frac{Et^3}{12 \rho V^2 D^3}$$

The characteristic velocity was selected as the snatch velocity, V_s , and the numerical factor of 12 was dropped (a valid step in dimensional analysis).

The expression then becomes

$$\Omega = \frac{E}{\rho V_s^2} \left(\frac{t}{D_0} \right)^3 \quad (1)$$

Furthermore, it was felt that canopy stiffness would be more analogous to plate bending stiffness than to beam bending stiffness, since the Poisson's ratio effect is neglected in the bending of beams, but is important in the bending of plates where lateral contraction is inhibited much more. Hence, the parameter E (Young's modulus) was replaced by the term $E/(1-\nu^2)$ giving the final form for the expression

$$\zeta = \frac{E}{\rho V_s^2 (1-\nu^2)} \left(\frac{t}{D_c} \right)^3 \quad (2)$$

This parameter is then similar dimensionally to the expression often used in plate theory, i.e., the work of Calligeros [21]. Certainly, a parachute canopy does not exhibit the stiffness exhibited by a plate in small deflection theory; nevertheless,

there must be some similarity between the unfolding of fabric and the bending of a plate. Furthermore, analysis shows that if only the overexpansion of the inflated canopy were considered, then the theory for strain in a hemispherical shell could be applied, and an expression of the form

$$\zeta' = \frac{E}{\rho V_s^2 (1-\nu)} \left(\frac{t}{D_0} \right)^3 \quad (3)$$

would result. Thus the difference between Eqs. (1), (2) and (3) is in the relative effect of Poisson's ratio on canopy rigidity.

The form of the parameter selected for study was

$$\zeta = \frac{E}{\rho V_s^2 (1-\nu^2)} \left(\frac{t}{D_0} \right)^3$$

This parameter will be called the "relative stiffness index."

Modification of Form for Relative Stiffness Index

The relative stiffness index given in Eq. (2) contains canopy design variables (E, ν, t, D_0) and drop condition variables (ρ, V_s). More insight into the effect of each parameter may be obtained by modifying the expression as follows: If the Froude number is introduced, the expression can be changed from

$$\zeta = \frac{E}{\rho V_s^2 (1-\nu^2)} \left(\frac{t}{D_0} \right)^3$$

using $Fr = \frac{V_s^2}{gD_0}$ or $V_s^2 = gD_0 Fr$ into

$$\zeta = \frac{E}{(1-\nu^2)} \left(\frac{1}{\rho g Fr} \right) \left(\frac{t^3}{D_0^4} \right)$$

Multiplying the numerator and denominator by the parachute *canopy* weight, W_p , and rearranging gives

$$\zeta = \frac{E}{W_p (1-v^2)} \left(\frac{1}{Fr} \right) \left(\frac{W_p}{g \rho D_o^3} \right) \left(\frac{t^3}{D_o} \right)$$

Since $W_p/g = m_p$, the parachute *canopy* mass, and defining $M_{r,p} = \frac{m_p}{\rho D_o^3}$ as

done by Lee [9], gives

$$\zeta = \left(\frac{E}{(1-v^2)} \right) \left(\frac{t^3}{W_p D_o} \right) \left(\frac{M_{r,p}}{Fr} \right) \quad (4)$$

Using $w_c = \frac{W_p}{(\pi D_o^2/4)}$ for the average areal density of the canopy gives $W_p = \pi D_o^2 w_c/4$.

Substituting this into Eq. (4) gives

$$\zeta = \left(\frac{4}{\pi} \right) \left(\frac{E}{(1-v^2)} \right) \left(\frac{t^3}{w_c D_o^3} \right) \left(\frac{M_{r,p}}{Fr} \right)$$

Dropping the $4/\pi$ term since it is just a constant like the value of 12 from plate bending theory gives the final form

$$\zeta'' = \left[\frac{E}{(1-v^2) w_c} \left(\frac{t}{D_o} \right)^3 \right] \left(\frac{M_{r,p}}{Fr} \right)$$

The term in brackets is a function only of the parachute construction, while the expression in parentheses includes the effect of drop conditions, as well as canopy mass and size.

We can define a modified canopy stiffness index, call it η' , different from Heinrich's stiffness index[†] (but related to it) as follows:

$$\eta' = \frac{E}{w_c} \left(\frac{1}{(1-\nu^2)} \right) \left(\frac{t}{D_0} \right)^3 \quad (5)$$

With this definition, the relative stiffness index parameter becomes

$$\zeta'' = \eta' \left(\frac{M_{r,p}}{Fr} \right) \quad (6)$$

Physical Significance of Relative Stiffness Index

Examination of Eq. (6) for the relative stiffness index term will show the importance of each variable physically. This equation shows how the relative stiffness index fits in with the complete picture of relative canopy rigidity. The Froude number term in the denomination makes the "absolute" or "geometric" stiffness into a "relative" stiffness, since it is now relative to inertia and gravity forces during opening. The term in the numerator $M_{r,p}$ is proportional to the ratio of canopy mass to included mass: $m_p/\rho D_0^3$. The importance of this term was also recognized by Kaplun [1] as early as 1951. He called this term the "canopy inertia number," I , defined as

$$I = \frac{m}{\rho D^3}$$

where m was the mass of the parachute *canopy* (Kaplun's study dealt with "infinite mass" inflations only, thus the payload mass did not enter the study as a variable). Kaplun felt that it was

[†] Heinrich's stiffness index was defined as $\eta = \left(\frac{D_{max}}{D_0} \right) \left(\frac{W_c}{S_0 W_{cl}} \right)$. Since $D_{max} = f(E, \nu, t, D_0)$, the stiffness indices are obviously related in some physical way, but in a way probably not determinable by any simple mathematical analysis.

...particularly important to establish the effect of the inertia number, since an opening governed by canopy inertia forces would be characteristically different from one in which the mass of the canopy has no effect. In the former case, the rate of opening would be determined by the dynamic pressure and the inertia of the canopy, while in the latter case by the volume in flow of air. It is the latter, flow-determined case which has been assumed by O'Hara and by W. Müller in the rational analyses which they respectively suggested.

Thus, the relative stiffness index of Eq. (2) includes the effect of canopy inertia as well. To the author's knowledge, the present study is the first one to identify the importance of the variables in the combination shown in Eq. (6).

Overview

The next step of the present study, then, is to examine available parachute test data to see if stiffness effects can be correlated using the relative stiffness index of Eq. (2). The study will be based primarily on the experimental data of Lee [9,22], as this is the only data to the author's knowledge where several different fabric densities were tested on several parachute scales as well. A small amount of wind tunnel test data will also be examined, as well as some full-scale drop tests, which were conducted using similar parachutes constructed with fabrics of different areal densities.

In order to conduct the desired data correlation studies, it is first necessary to develop data for the parachute fabric properties needed in the relative stiffness index. This task involves obtaining data for Young's modulus and Poisson's ratio for various parachute fabrics and will be examined in the next section of this report.

EVALUATION OF FABRIC PROPERTIES

To use the relative stiffness index it is necessary to have values of Young's modulus, E , and Poisson's ratio, ν , for parachute fabric. To truly characterize the properties of parachute fabric, it must be considered as a nonlinear material with complex strain, strain rate, and hysteresis properties. If the fabric is assumed to behave *linearly*, the general stress-strain relationships for any linearly elastic, *anisotropic* material must be represented by six equations which relate the six most general components of strain to the six components of stress.

Somewhat less complicated representations of fabric properties have been conducted by Steeves [23], and by Remington, Madden, and O'Callahan [24]. However, these models were for specialized applications, and still too complex to use for this study of scaling parachute stiffness. Since fabrics are not isotropic materials, strictly speaking, there is no single value of E and ν that can be used to characterize fabric properties. However, what is needed is some type of *estimate* for parachute cloth in order to apply the method.

Fabric data from several sources were examined and estimates for E and ν attempted. Since parachute fabric is stressed biaxially during canopy opening and descent; it would be desirable ideally to obtain these values from biaxial test data for each particular fabric of interest. Both biaxial and uniaxial test data were examined and isotropic and orthotropic models for fabric properties were each evaluated.

Biaxial Test Data

The most consistent results for both Young's modulus, E , and Poisson's ratio, ν , were obtained from biaxial test data obtained for 50 g/m^2 (1.47 oz/yd^2) plain weave British nylon parachute fabric, and reported by Render and Bradley [25].

The fabric was *assumed* to behave isotropically, in which case the strain equations in the two directions would be given by

$$\epsilon_1 = \frac{1}{E}(\sigma_1 - \nu\sigma_2)$$

$$\epsilon_2 = \frac{1}{E}(\sigma_2 - \nu\sigma_1)$$

These equations were solved for E and ν to give

$$E = \frac{\sigma_1^2 - \sigma_2^2}{\sigma_1\epsilon_1 - \sigma_2\epsilon_2} \quad (7)$$

$$\nu = \frac{\sigma_2\epsilon_1 - \sigma_1\epsilon_2}{\sigma_1\epsilon_1 - \sigma_2\epsilon_2} \quad (8)$$

Eight test points were chosen at random from the biaxial stress-strain data as reported by Render and Bradley and these points are shown on their plot in Fig. 5. Notice that some data points at negative values of strain were also taken.

The data were substituted into Eqs. (7) and (8) and the results obtained are shown in Table 1. It can be seen that the data are fairly consistent, and the standard deviations obtained are reasonable under the circumstances. This led to confidence that this method would work for other fabrics.

Table 1. Properties of 1.47 oz/yd² plain weave, British nylon parachute fabric

Point Selected (see Fig. 5)	Young's Modulus E N/mm	Poisson's Ratio ν
1	38.5	0.154
2	33.9	0.228
3	35.5	0.346
4	40.5	0.215
5	41.7	0.095
6	39.3	0.130
7	41.5	0.225
8	36.4	0.273
Arrange values:	38.4 N/mm	0.208
Standard deviation:	2.9 N/mm	0.081

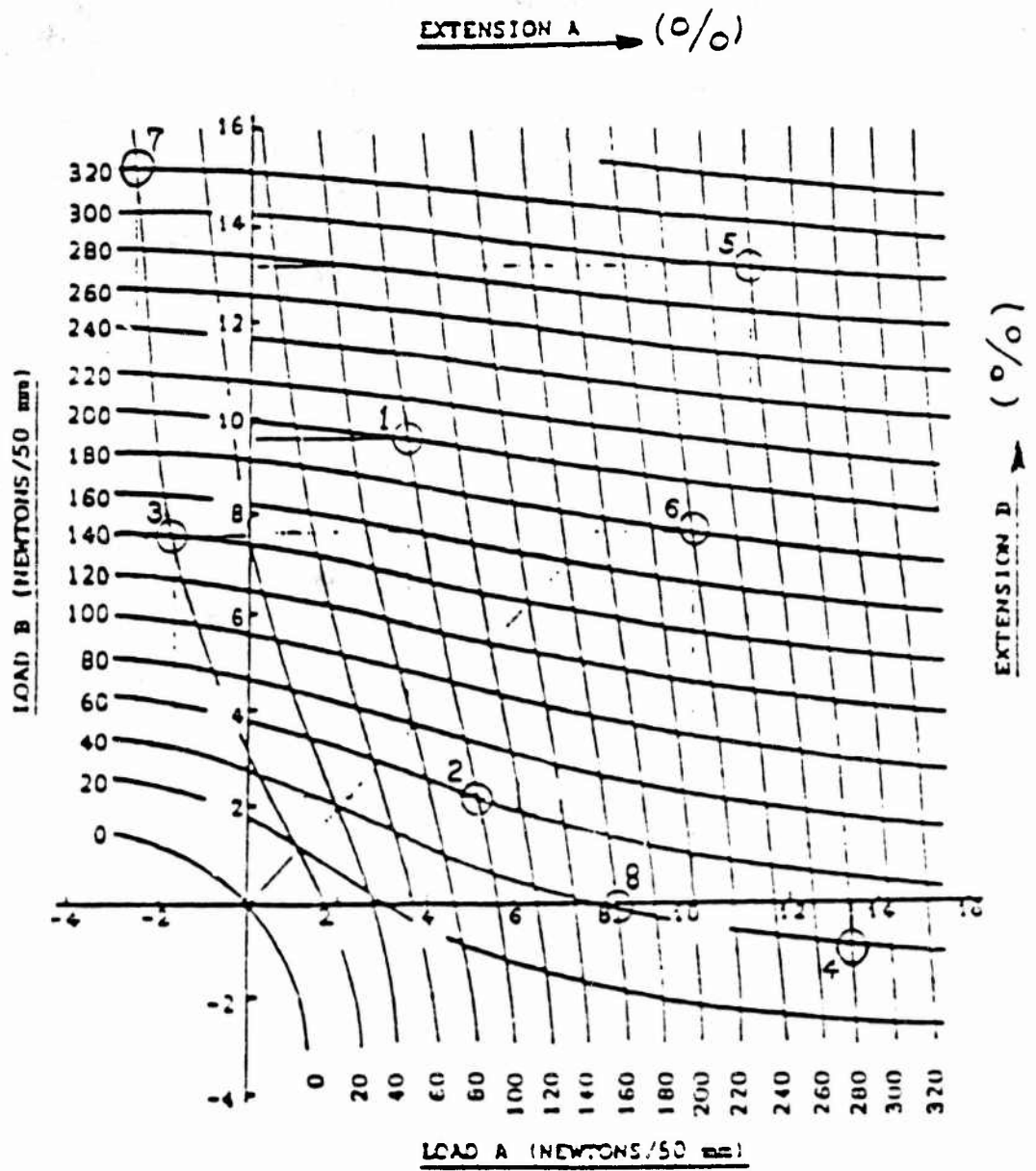


Fig. 5: Biaxial stress-strain relationships for 50 g/m² plain weave British nylon parachute fabric.
(Figure taken from Ref. 25)

A similar approach was tried on the biaxial stress strain data for four fabrics tested by Monego and Pilsworth [26] using a pressurized cloth cylinder for the tests. It was hoped that this technique would yield values for heavier fabrics that could be used to estimate Poisson's ratio for the heavy fabrics used for the parachute drop tests reported by Lee. Unfortunately, the *isotropic* stress strain equations would not give meaningful values of Young's modulus or Poisson's ratio for any of the heavier fabrics. It was next decided to look at uniaxial test data.

Uniaxial Fabric Test Data

From the [26] test data for *uniaxial* tests to failure on conventional weight parachute fabric, it was possible to obtain separate values for stiffness in the warp and fill directions. Assuming a fabric thickness of 0.0028 in as measured in Lee's later tests, the following secant modulus values were obtained:

$$E_{\text{warp}} = 7.80 \times 10^4 \text{ psi}$$

$$E_{\text{fill}} = 5.81 \times 10^4 \text{ psi}$$

$$E_{\text{ave}} = 6.8 \times 10^4 \text{ psi}$$

An order of magnitude for Poisson's ratio for this fabric was assumed by *modifying* the isotropic equations to the following form:

$$\epsilon_w = \frac{\sigma_w}{E_w} - \frac{\nu \sigma_f}{E_f} \quad (9)$$

$$\epsilon_f = \frac{\nu \sigma_w}{E_w} - \frac{\sigma_f}{E_f} \quad (10)$$

The use of two different values of Young's modulus in this form of equation violates the isotropic assumptions on which the equations are based. However, use of these equations on four test data points at stress ratios of $\frac{\sigma_w}{\sigma_f} = \frac{1}{1}$ and $\frac{\sigma_w}{\sigma_f} = \frac{2}{1}$ gave values of Poisson's ratio in the range from $0.045 \leq \nu \leq 0.270$, with an average value

of $\nu = 0.14$. This value compares favorably with the value of 0.21 for the British parachute fabric.

Linear, Orthotropic Fabric Model

Because the above technique yielded some promising values for Poisson's ratio, it was decided to model the fabric more accurately using the following linear orthotropic stress-strain relations:

$$\epsilon_x = S_{11}\sigma_x + S_{12}\sigma_y \quad (11)$$

$$\epsilon_y = S_{21}\sigma_x + S_{22}\sigma_y \quad (12)$$

In this model, S_{11} and S_{22} can be different from each other, but it is required that $S_{12} = S_{21}$. The *isotropic* equations, arranged in similar form, are

$$\epsilon_x = \left(\frac{1}{E}\right)\sigma_x + \left(\frac{-\nu}{E}\right)\sigma_y$$

$$\epsilon_y = \left(\frac{-\nu}{E}\right)\sigma_x + \left(\frac{1}{E}\right)\sigma_y$$

Comparing these equations with Eqs. (11) and (12) shows that the orthotropic model allows the use of separate values of Young's modulus in the warp and fill directions, but the requirement that $S_{12} = S_{21}$ would require the use of a term like $\frac{-\nu_{ave}}{E_{ave}}$ for S_{12} and S_{21} .

The values of S_{11} and S_{22} would come from uniaxial fabric tests in the warp and fill directions and we would then try to represent the fabric properties as

$$\epsilon_w = \left(\frac{1}{E_w}\right)\sigma_w - \frac{\nu_{ave}}{E_{ave}}\sigma_f \quad (13)$$

$$\epsilon_f = \frac{-\nu_{ave}}{E_{ave}}\sigma_w + \left(\frac{1}{E_f}\right)\sigma_f \quad (14)$$

Using the values of E_w , E_f , and E_{ave} from the uniaxial test data, the equations given above were applied to both the pressurized cylinder and cruciform test data

for the MIL-C-7020-1 parachute fabric and the results are given in Table 2. Note that the value of 0.142 from Table 2 compares favorably with the value of 0.14 reported earlier using Eqs. (9) and (10).

Table 2. Values of Poisson's ratio for MIL-C-7020-1 type parachute fabric using Eqs. (13) and (14)

Test Type	Poisson's Ratio, ν
Cruiform, $\frac{\sigma_w}{\sigma_f} = 1.0$, Warp	0.0880
Cruiform, $\frac{\sigma_w}{\sigma_f} = 1.0$, Fill	0.234
Press. Cyl, $\frac{\sigma_w}{\sigma_f} = 1.0$, Warp	0.170
Press. Cyl, $\frac{\sigma_w}{\sigma_f} = 1.0$, Fill	0.0638
Cruiform, $\frac{\sigma_w}{\sigma_f} = 2.0$, Warp	0.210
Cruiform, $\frac{\sigma_w}{\sigma_f} = 2.0$, Fill	0.038
Press. Cyl, $\frac{\sigma_w}{\sigma_f} = 2.0$, Warp	0.207
Press. Cyl, $\frac{\sigma_w}{\sigma_f} = 2.0$, Fill	0.129
Average Value:	0.142

An attempt to use this approach (modified orthotropic equations) for the body armor fabric of [26] was tried, but the values obtained for Poisson's ratio seemed unreasonable.

The final choice for values of Young's modulus was based on uniaxial test data obtained for samples of the cloth used to construct the parachutes used in each of Lee's drop tests. Average values from tests in the warp and fill directions were used for each of the fabric weights given in Table 3 below.

Table 3. Uniaxial test data for Young's Modulus and average values used for analysis

Actual Fabric Areal Density, oz/vd ²	Fabric Thickness, in	E _{warp} (psi)	E _{su} (psi)	E _{ave} (psi)
0.94	0.0028	7.80 x 10 ⁴	5.81 x 10 ⁴	6.80 x 10 ⁴
4.1	0.011	5.40 x 10 ⁴	4.73 x 10 ⁴	5.06 x 10 ⁴
9.2	0.021	7.06 x 10 ⁴	4.50 x 10 ⁴	5.78 x 10 ⁴
12.2	0.027	3.10 x 10 ⁴	2.05 x 10 ⁴	2.58 x 10 ⁴

The final input values to the relative stiffness index were to use the values of average Young's modulus from the table above for each individual fabric, and a common value of Poisson's ratio $\nu = 0.14$ for all fabrics.

Ordinary changes to the value of Poisson's ratio for the different fabrics, if the values could be found, would have negligible effect on the final numerical value of relative stiffness index. The scatter in experimental data would obscure any attempt to verify the Poisson's ratio effect accurately.

APPLICATION OF METHOD TO EXPERIMENTAL DATA CORRELATION

C-9 Parachute Test Data

The most systematic experimental study of the effects of fabric stiffness on parachutes of various sizes is the work done by Lee [9,22]. In [9], Lee reports the results of drop tests conducted on full-scale 28 ft diameter, solid cloth C-9 parachutes, as well as for a 14 ft diameter $1/2$ -scale model and a 7 ft diameter $1/4$ -scale model. The three parachutes were constructed of 1.1 oz/yd² ripstop nylon.

In [22], Lee presents similar drop test data on full-scale and $1/4$ -scale C-9 parachutes using fabric of the following weights: 1.1 oz, 4.1 oz, 9.2 oz, and 12.2 oz/yd². Lee presents data for non-dimensional opening force and non-dimensional opening time vs. Froude number, Fr , for two mass ratios.

A matrix of the test conditions is presented in Table 4.

Table 4. Range of test variables covered in Lee's tests

Scale	Actual Fabric Areal Density, oz/yd ²	Froude Number Range
$M_{r,1} = 0.13$ (Ref. 22)		
Full (C-9)	0.94	4-7
Full (C-9)	4.1	4.5-5
Full (C-9)	9.2	2-7.5
Full (C-9)	12.2	2.5-4.5
One-Quarter	0.94	3.5-50
One-Quarter	4.1	4-20
$M_{r,1} = 0.20$ (Ref. 9)		
Full (C-9)	0.94	4-6
One-Half	0.94	4-20
One-Quarter	0.94	4-60

All drop tests were done outside, from a crane for vertical drops, and from a packed configuration. Lee's test data are presented for opening time, as opposed to filling time. Opening time is here defined as the time from occurrence of first snatch force to the time of peak opening force (filling time is usually defined as the

time at which the canopy first reaches a projected area equal to the steady state projected area).

Opening Time Data Correlation, Mass Ratio 0.13

Fig. 6 is a composite plot of all the data presented in [22] for non-dimensional opening time, τ , vs. Froude number. It can be seen that the correlation shown is fair. The effects of fabric areal density relative to canopy diameter are somewhat difficult to sort out, but some conclusions can be reached.

The data points for the smallest parachute with a relatively heavy fabric ($1/4$ scale, 4.1 oz/yd^2) have the shortest non-dimensional opening time, falling below nearly all the other data. The data for the full-scale parachute using the lightest (1.1 oz/yd^2) fabric (and even with the 4.1 oz/yd^2 fabric) show the longest opening time. The $1/4$ -scale parachute with the light fabric and the full-scale parachutes with the heavy fabrics fall somewhere in the middle.

If all these data points are plotted against the relative stiffness index, ζ , the correlation shown in Fig. 7 results. It can be seen that this correlation is considerably better than that shown in Fig. 6.

Opening Time Data Correlation, Mass Ratio 0.20

Examination of Fig. 2 shows that a change in mass ratio from 0.13 to 0.20 would have only a very small effect on theoretical filling time, much less than the range of experimental data scatter for a given mass ratio. It is expected that the effect on opening time would be just as small.

With this logic in mind, the data from [9] for a mass ratio of 0.20 were plotted together with the mass ratio 0.13 data. This provides additional data points for the $1/4$ -scale and full-scale C-9 parachutes, as well as data for the $1/2$ -scale C-9 parachute. The correlation for non-dimensional opening time vs. relative stiffness index is shown in Fig. 8 (the flagged data points are for mass ratio 0.20). The correlation is still seen to be generally good. By contrast, if the other mass ratio is simply plotted vs. Froude number, the graph in Fig. 9 results.

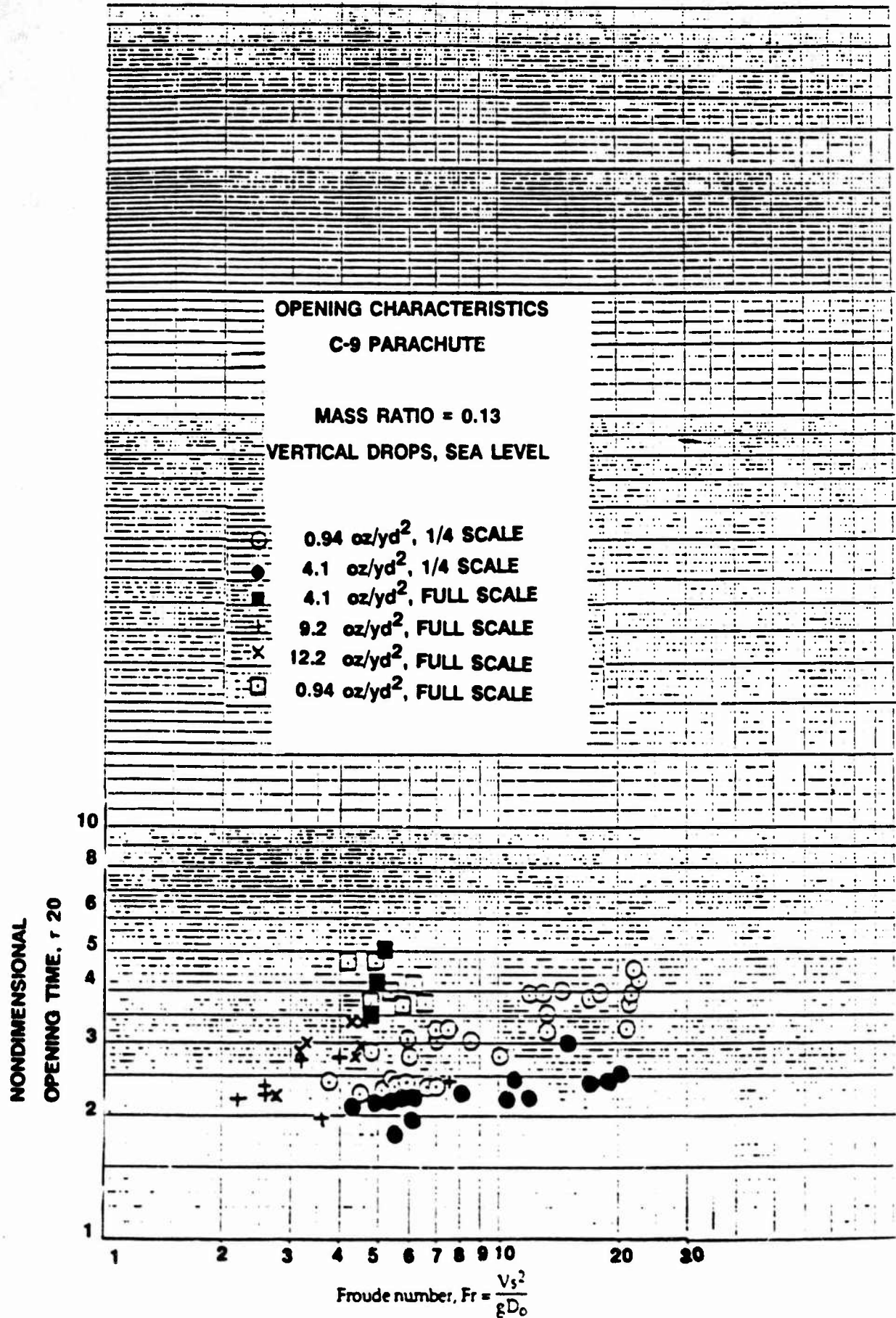


Fig. 6: Opening time as a function of Froude number for full-scale and 1/4-scale C-9 parachutes at mass ratio 0.13.

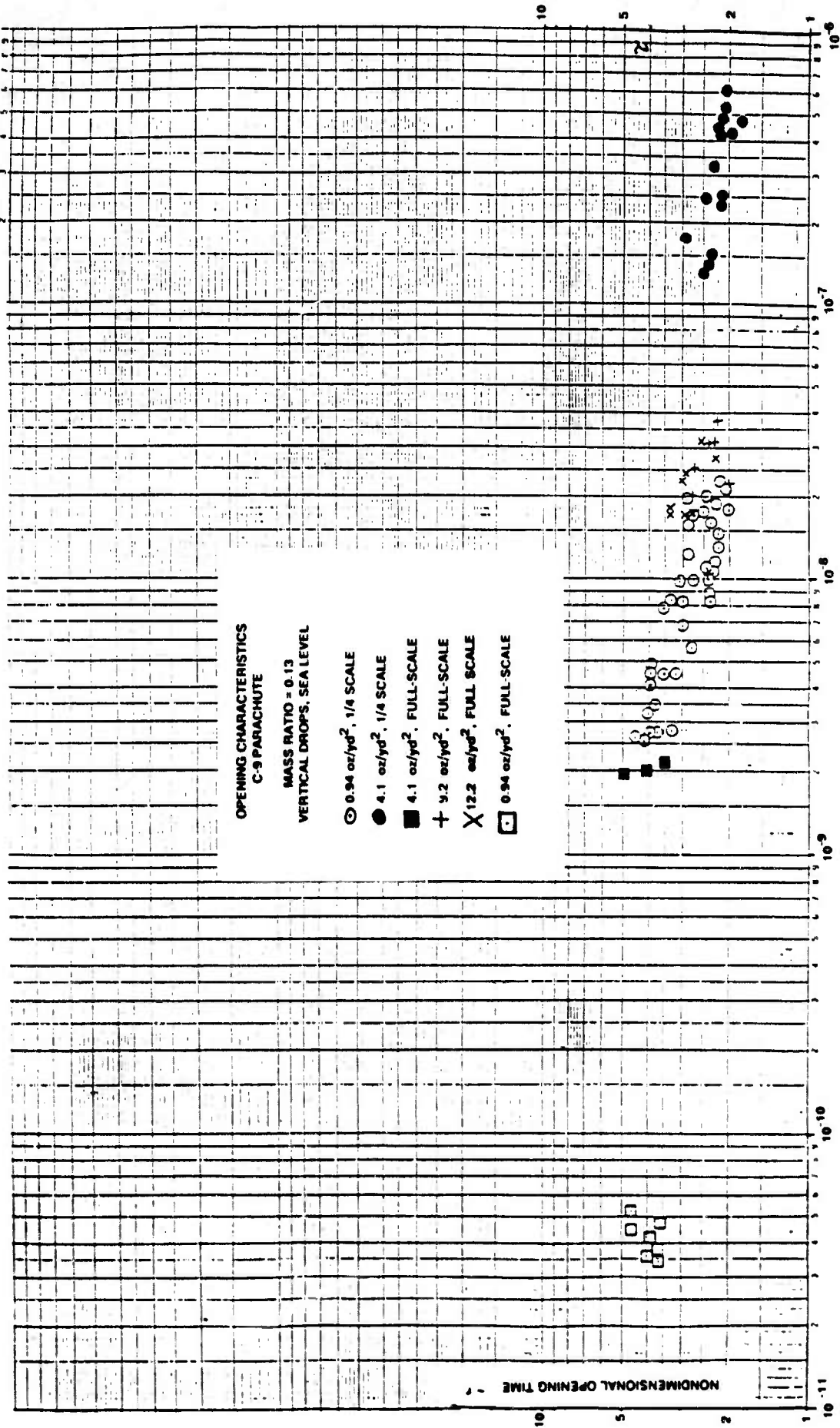


Fig. 7: Opening time as a function of relative stiffness index for full-scale and 1/4-scale C-9 parachutes at mass ratio 0.13. Relative stiffness index, $\zeta = \frac{E}{\rho V_s^2 (1-\nu^2)} \left(\frac{l}{D_0}\right)^3$

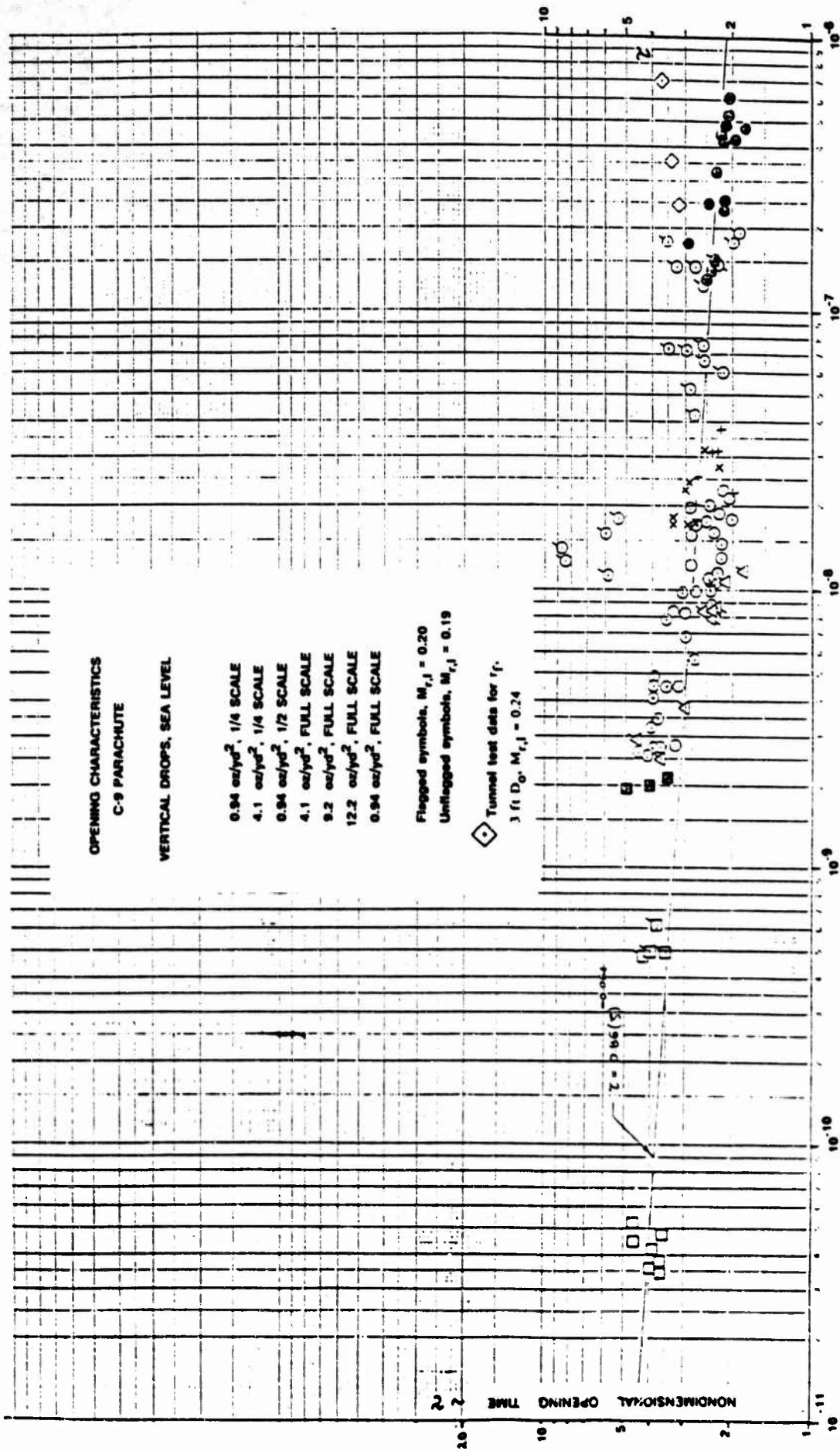


Fig. 8: Opening time as a function of relative stiffness index for full-scale 1/2-scale, and 1/4-scale C-9 parachutes at mass ratios 0.13 and 0.20.

$$\text{Relative stiffness index, } \zeta = \frac{E}{\rho V_S^2 (1-\nu^2)} \left(\frac{l}{D_0} \right)^3$$

**OPENING CHARACTERISTICS
C-9 PARACHUTE**

VERTICAL DROPS, SEA LEVEL

- 0.94 oz/yd², 1/4 SCALE
- 4.1 oz/yd², 1/4 SCALE
- △ 0.94 oz/yd², 1/2 SCALE
- 4.1 oz/yd², FULL SCALE
- + 9.2 oz/yd², FULL SCALE
- × 12.2 oz/yd², FULL SCALE
- ◻ 0.94 oz/yd², FULL SCALE

Flagged symbols, $M_{r,i} = 0.20$

Unflagged symbols, $M_{r,i} = 0.13$

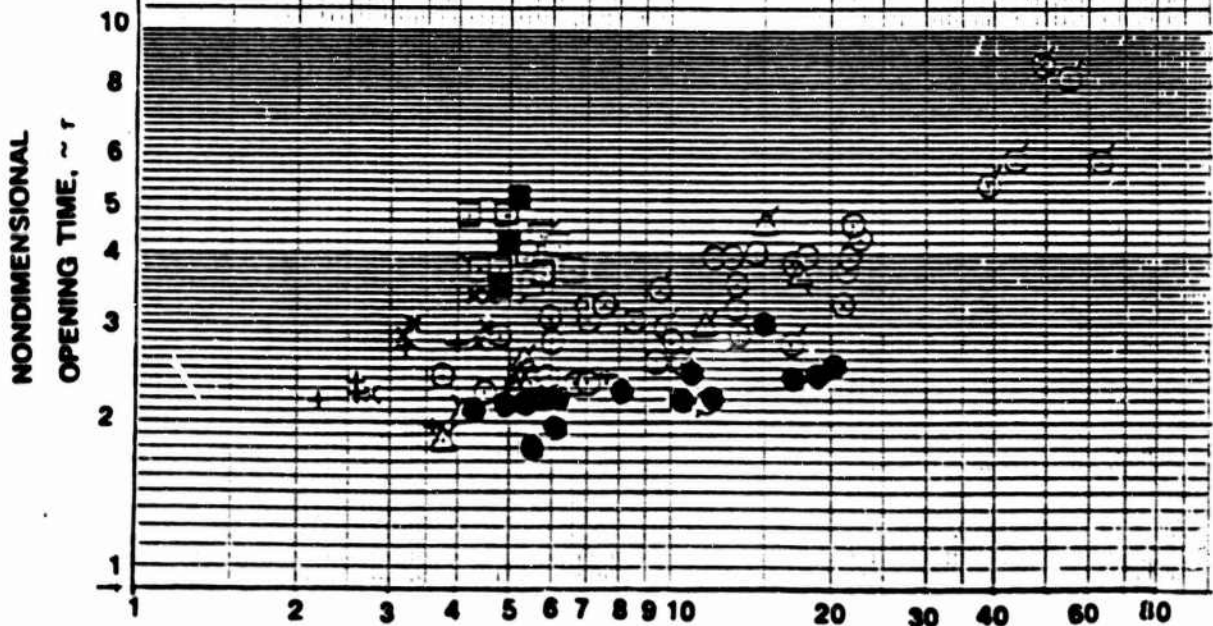


Fig. 9: Opening time as a function of Froude number for full-scale, 1/2-scale, and 1/4-scale C-9 parachutes at mass ratios 0.13 and 0.20.

$$\text{Froude number, } Fr = \frac{V_s^2}{g D_0}$$

In Fig. 8, there are a few data points that correlate poorly in the range $\zeta = 1.1 \rightarrow 1.8 \times 10^{-8}$. The reason for this is not known. Note, however, that the $1/2$ -scale data fit nicely between the $1/4$ -scale and full-scale data. The main interesting trend shown here experimentally agrees with Fu's theory in that there is no discernable difference between the two mass ratios, and that the effects of parachute scale and fabric stiffness are greater than the effects of change in mass ratio.

Wind Tunnel Data

In [20], Heinrich presents test data for small-scale wind tunnel models of the C-9 parachute that were 3 ft in diameter. A finite mass test was simulated by using a suspended mass attached to a cable. As the parachute opened in the wind tunnel, it moved downstream in the tunnel, simultaneously lifting the mass. The mass ratio used was 0.24, again close enough to the values of 0.13 and 0.20 previously plotted, considering experimental data scatter.

Heinrich measured filling time as the point where projected canopy area first equals steady state projected area. The data points are shown on Fig. 8. The points fall just above the data points for the 4.1 oz/yd², $1/4$ - scale C-9 canopy, but if the opening time were known as opposed to the filling time, the points would be even closer to the other data points. The difference between these values and the other values may also be due to two other reasons: the manner in which the wind tunnel test is conducted makes it difficult to simulate a vertical drop test, and at this small a scale factor (approximately $1/10$), the effect of reinforcing along the parachute top cord lines may overshadow the basic stiffness characteristics of larger, solid flat circular parachutes.

It is interesting to note that all the data points on Fig. 8 are correlated fairly well by the equation:

$$\tau = 0.86(\zeta)^{-0.064} \quad (15)$$

This equation covers the complete range of mass ratios and Froude numbers considered in all C-9 tests discussed to this point.

Application of the Method to 35 ft D_0 T-10 Parachutes

Watson [27] presents test data for a series of drop tests for the 35 ft diameter T-10 parachute. A series of 46 or more drops were conducted from aircraft at altitudes ranging from approximately 800 ft to 38,000 ft; snatch velocities varying between 200 and 475 fps; and suspended loads ranging from 174 to 865 lb. Two types of canopy construction were used: a standard 1.1 oz/yd² (nominal) T-10 canopy, and a high-strength (2.25 oz/yd²) extended skirt canopy. Various trajectory deployment angles were also tested.

Watson's data were not presented in dimensionless form, so it was necessary to convert the data into the format desired. In addition, the time data were not presented as an opening time (time from snatch force to peak force), but as a filling time (time to first full-open projected area). Therefore, a non-dimensional *filling* time, τ_f , was plotted vs. the stiffness parameter, ζ .

The data are presented in Fig. 10, together with one data point obtained on a 1/10-scale model wind tunnel test conducted by Heinrich [28] at finite mass conditions. The data correlation in this case does not follow the same trend as shown in Fig. 8, that is, a decreasing value of τ with increasing relative stiffness index, ζ . As a matter of fact, except for the single point for the wind tunnel test, it appears that the non-dimensional filling time is essentially constant—independent of stiffness index, payload mass ratio, or trajectory inclination angle.

To explore this phenomenon further, Watson's original data were replotted several different ways. Watson's original plot of filling time vs. snatch velocity is reproduced as Fig. 11. Here it can be seen that filling time decreases as snatch velocity increases. It can be seen that the high strength canopy has a slightly longer filling time than the conventional T-10 canopy. When the same data are non-dimensionalized, a plot of non-dimensional filling time, t_f , vs. Froude number $Fr = V_s^2/gD_0$ is obtained, as shown in Fig. 12. It now appears that the parachute inflations show the constant (non-dimensional) filling time characteristic pointed out by earlier investigators.

To further sort out any trends, the data were replotted once more in Fig. 13, where non-dimensional filling time is plotted vs. "Froude number of operation,"

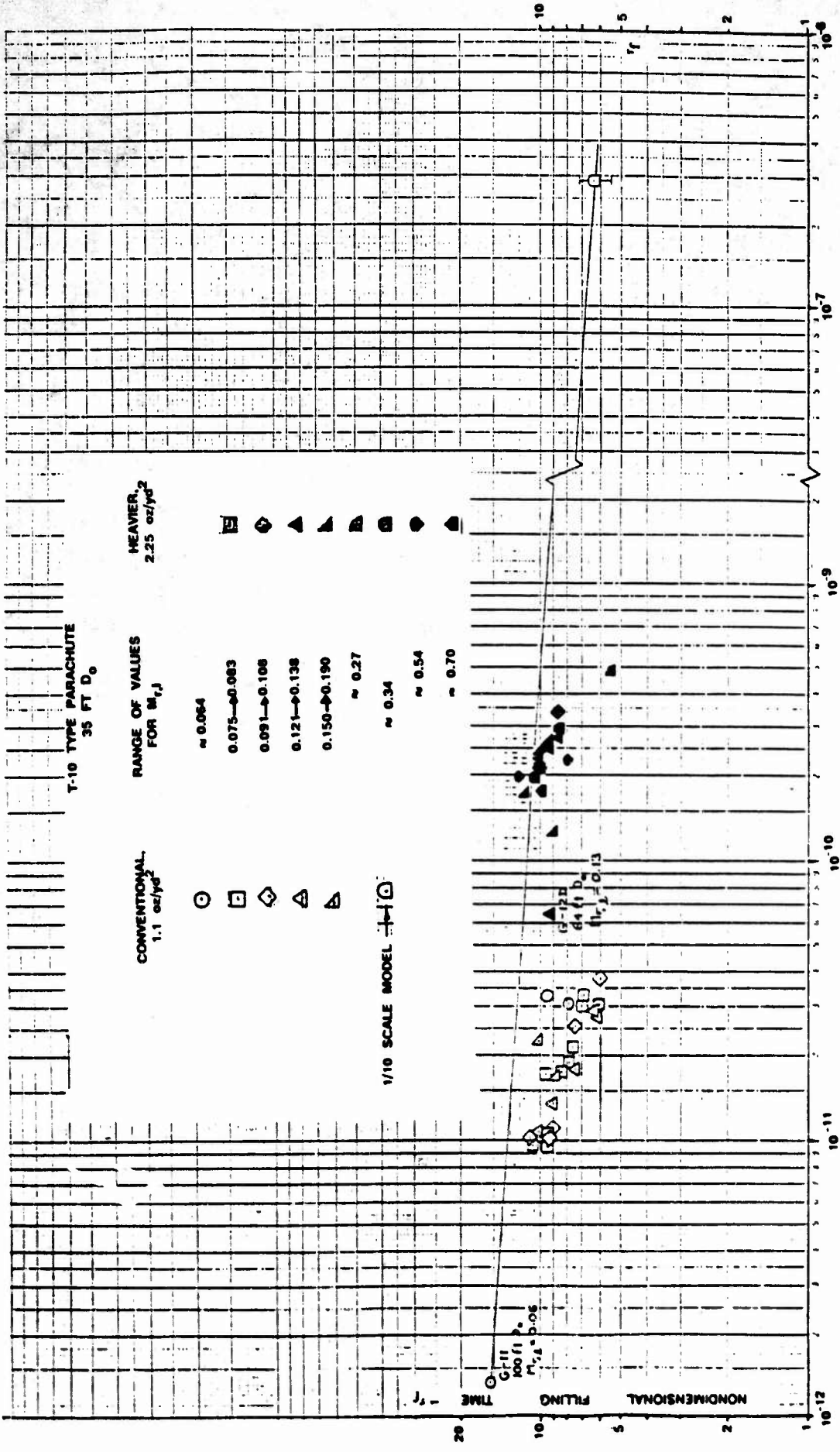


Fig. 10. Nondimensional filling time as a function of relative stiffness index for T-10 and other parachute configurations.

$$\text{Relative stiffness index, } \zeta = \frac{E}{\rho V_s^2 (1-u^2)} \left(\frac{t}{D_0} \right)^3$$

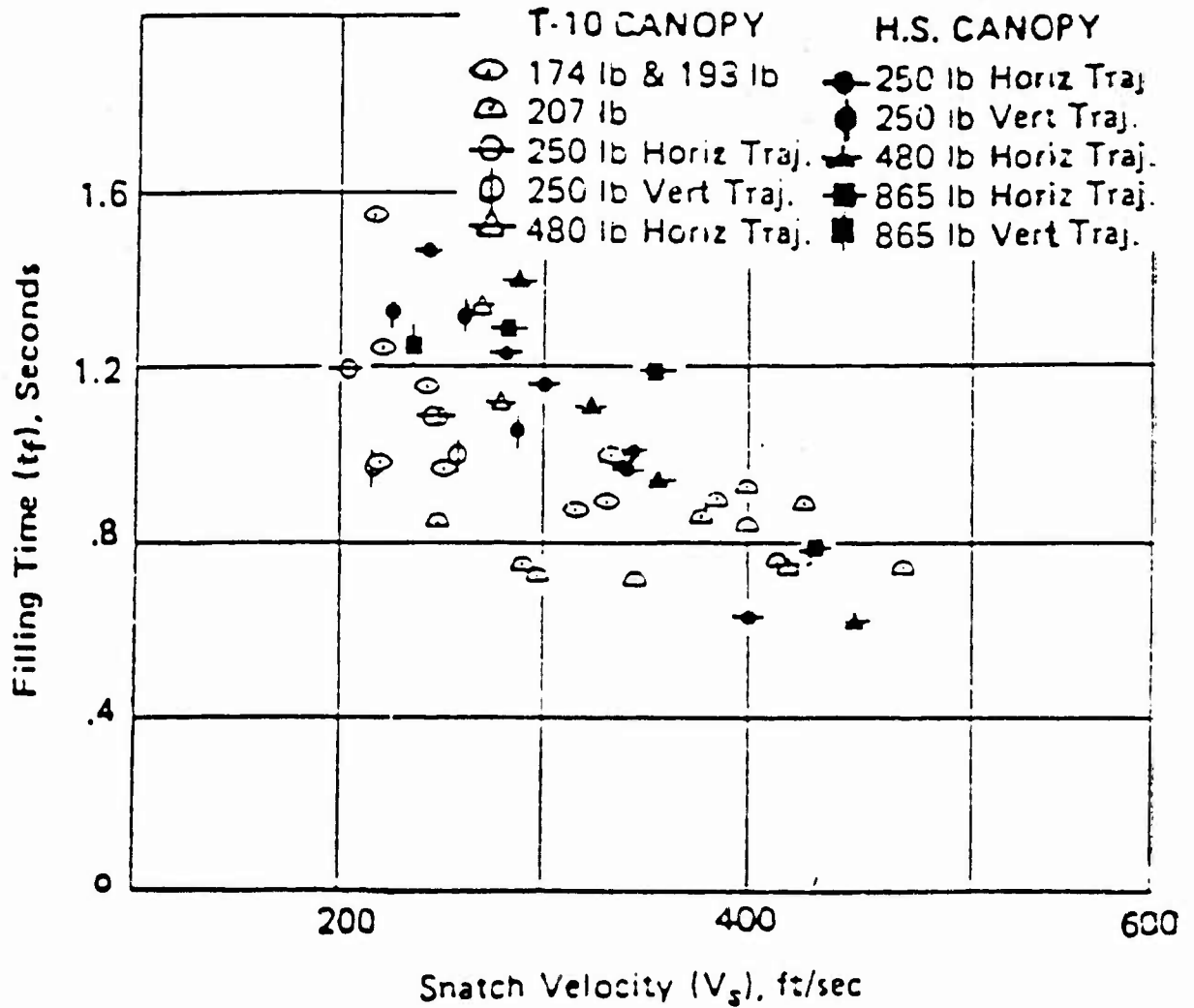


Fig. 11: Filling time vs. snatch velocity for T-10 extended skirt canopy and high strength canopy.
 35 ft. D_0 extended skirt canopy and high strength canopy.
 (Figure taken from Ref. 27)

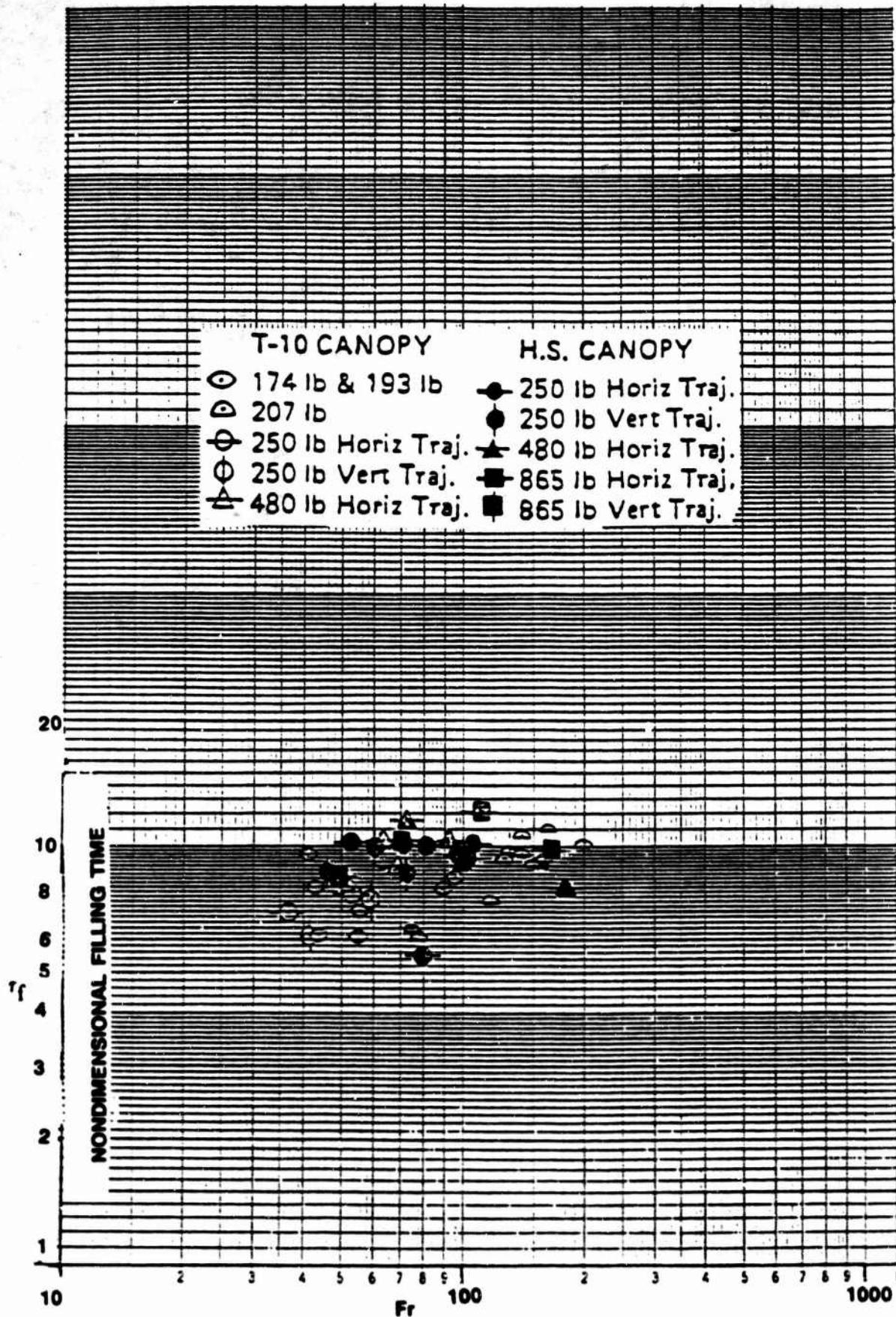


Fig. 12: Non-dimensional filling time vs. Froude number for T-10 extended skirt canopy and high strength canopy.

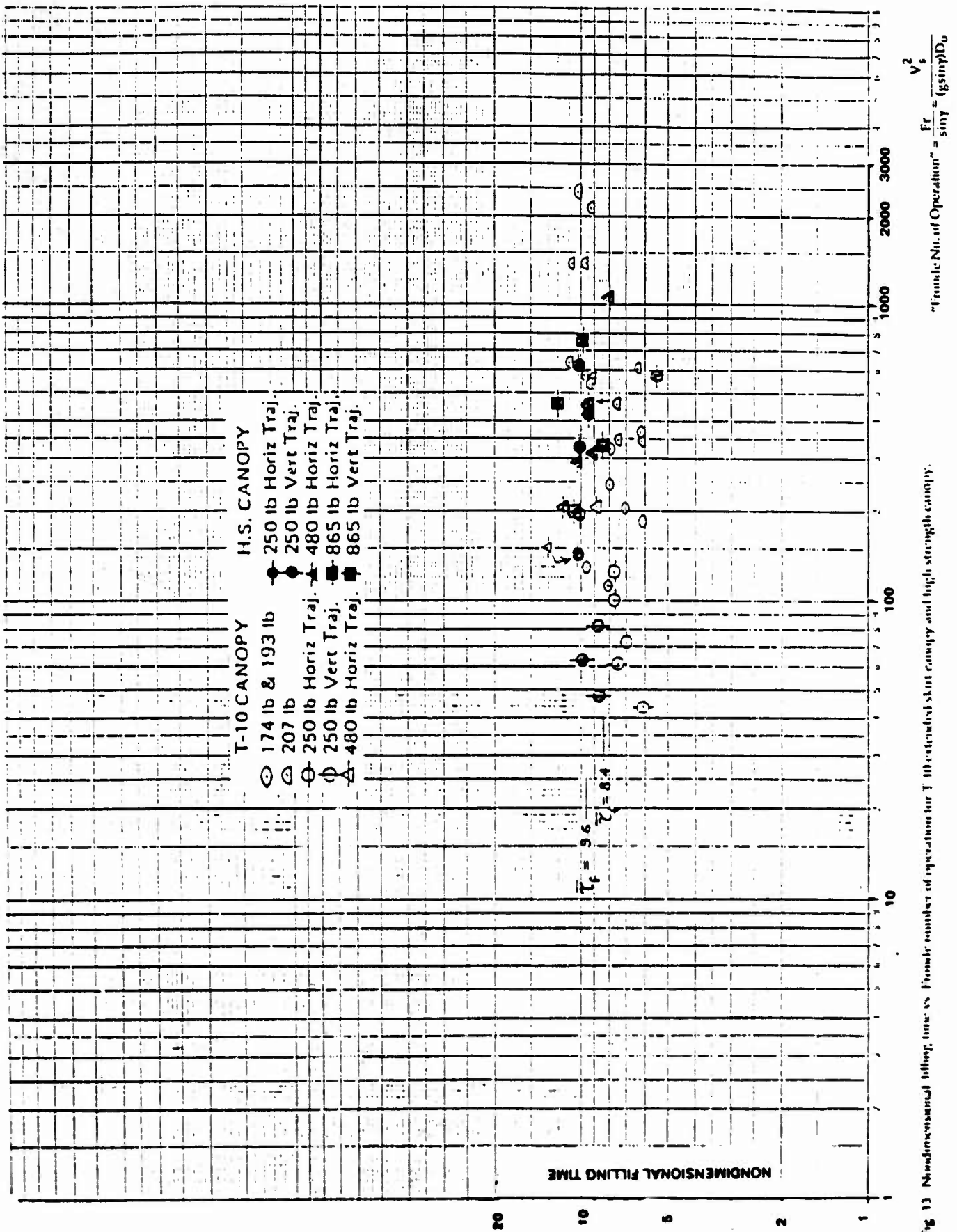


Fig 13 Nondimensional filling time vs Frankle number of operation for T-10 extended skirt canopy and high strength canopy.

$Fr/siny$. In this manner, the horizontal scale is expanded, but no new trends are observed. The flight path angles at deployment ranged from "horizontal deployments" with trajectory snatch angles as flat as 4° below horizontal, to "vertical deployments" with trajectory snatch angles as steep as 75° below horizontal. The filling time appears to be independent of snatch angle when non-dimensionalized vs. Froude number of operation.

Payload mass ratios for these tests varied from as low as 0.063 to as high as 0.70. The non-dimensional opening time being independent of mass ratio agrees with Fu's theoretical results for the C-9 parachute shown in Fig. 2. Here filling time is essentially independent of mass ratio for mass ratios above approximately 0.1. It is expected that the T-10 parachute would show the same general characteristics.

The only parameter that seemed to affect filling time in a statistically significant way was the fabric density. The shaded symbols for the heavier (2.25 oz/yd²) construction show a longer filling time than the standard 1.1 oz/yd² fabric. The average non-dimensional filling times are $\bar{\tau}_f = 8.4$ for the standard construction parachute, based on 28 tests; and $\bar{\tau}_f = 9.6$ for the heavier construction parachute, based on 18 tests. These values are shown on Fig. 13. Note, however, that the data scatter within *either* set of fabric tests is greater than the difference between the two mean values.

Going back to the T-10 data correlation shown in Fig. 10 and comparing it with the C-9 correlation shown in Fig. 8, it appears that there was not enough variation in the relative stiffness index ζ to show any trend for the T-10 parachute. This was primarily because the variation in parachute and test conditions did not cover a wide enough range. The thickness to diameter ratio of the parachutes varied only from 6.7×10^{-6} to 1.6×10^{-5} , as opposed to from 8.3×10^{-6} to 1.3×10^{-4} for Lee's C-9 type drop tests.

It is interesting to note that passing a line through the T-10 wind tunnel data point and using the same slope as the line on the C-9 data plot correlates the T-10 tunnel test point well with the full-scale data. This line is shown in Fig. 10.

Large Diameter Parachutes (G-12 and G-11)

Test data were available to plot single points for the 64 ft D_0 G-12D parachute and the 100 ft D_0 G-11 parachute. The available data were incomplete for each of these parachute drops, and specification values had to be used for fabric properties, rather than actual values from measurements. Filling times rather than opening times were non-dimensionalized and plotted in Fig. 10. Drop altitudes also had to be estimated.

The G-12D data point (2.25 oz/yd² fabric) falls midway between the two groups of data shown for the T-10 parachutes. The payload mass ratio for this drop was 0.13, within the range of mass ratios covered by the T-10 drop tests. For the G-12D diameter and fabric weight used, the performance of this parachute puts it into the area of constant non-dimensional filling time, based on one data point.

The data point for filling time of the 100 ft D_0 G-11 parachute was for a payload mass ratio of 0.06. This is somewhat lower than the lower mass ratios tested for the T-10 parachute, but the data point is seen to fall along an extension of the line connecting filling time for the T-10 wind tunnel model with filling time for the heavier fabric T-10 prototypes.

OPENING SHOCK CORRELATION PARAMETERS

The approach initially taken for analyzing parachute opening shock during filling was the same as that used to analyze opening time. Available theories were used as a guide to interpreting test data. The scatter in test data for nominally identical drop conditions again makes it difficult to sort out trends unless test parameters are changed significantly, almost drastically.

A review of Figs. 3 and 4 from theory show that mass ratio and Froude number have a significant effect on non-dimensional opening shock. Fig. 2 shows that these parameters have a small effect on opening time. For this reason, it might be expected that the correlation parameters for stiffness effects might affect opening shock differently than for opening time.

Correlation Study for Opening Shock

Several different approaches were tried to correlate opening shock force to parachute canopy stiffness. Most of these attempts were unsuccessful. The first attempt was to correlate non-dimensional opening shock directly with the relative stiffness index, ζ . Since opening time correlated well with relative stiffness index, it was expected that opening shock would correlate well also. It turned out that the correlation was unsatisfactory.

A number of other attempts were tried for various correlations using modifications of the relative stiffness index, for example, raising the ratio of fabric thickness to parachute diameter, t/D_0 , to the first or second power, instead of to the third power. None of these attempts were successful either.

Since the peak opening load occurs during the last portion of the opening time interval, it may be affected differently by parachute line elasticity and canopy elasticity than opening time. Much of the time during inflation the forces in the suspension lines and canopy are relatively low. It is only during the final moments of inflation that the suspension line and canopy forces become large. This fact would explain the difference in the way mass ratio and Froude number affect opening shock as opposed to affecting opening time.

Effect of Suspension Line Elasticity

Goodrick [29] made a simplified study of the effects of installing a spring and damper between a parachute and its payload. This study assumed that the parachute was already initially fully inflated at the snatch velocity. He studied the effect of numerical variation in the spring constant and damper coefficient on peak opening shock load. In this manner, the filling time, τ_f , was set at zero, but different values of opening shock occurred for varying payload mass, snatch velocity and simulated suspension characteristics. It was found that the shock experienced by the payload was affected greatly by the simulated suspension characteristics.

In Payne's theoretical study [14], suspension line elasticity was varied together with initial suspension line stretch, and it was found that the canopy opening characteristics were affected by these values. Payne's theory was the first one to predict the characteristic two peaks in the force-time history. It was found that riser and shroud line stiffness and initial stretch have a significant effect on opening history and loads.

Modified Impulse Concept

The basic physics of the canopy opening process and payload deceleration dictate the following. The payload mass, snatch velocity, and terminal velocity are the only quantities that determine the total retarding impulse that must be applied to the payload to decelerate it to the desired velocity. Neglecting payload drag, the required impulse can be achieved by a large retarding force occurring over a short period of time, or a smaller retarding force occurring over a longer period of time. This principle, applied to the payload itself, is irrespective of canopy or suspension line elasticity, etc. However, the canopy and suspension line elasticity, canopy mass and drag, etc., all determine the nature of the force vs. time history.

Examination of Fig. 14, reproduced from [22], clearly shows this effect. At a given Froude number and mass ratio, the full-scale parachute with the 4.1 oz/yd² fabric has the largest non-dimensional opening time, but the smallest non-dimensional opening shock. The 1/4-scale, 4.1 oz/yd², parachute has the shortest

1/4-SCALE FULL-SCALE

○ 0.94 oz/yd²
● 4.1 oz/yd²

■ 4.1 oz/yd²

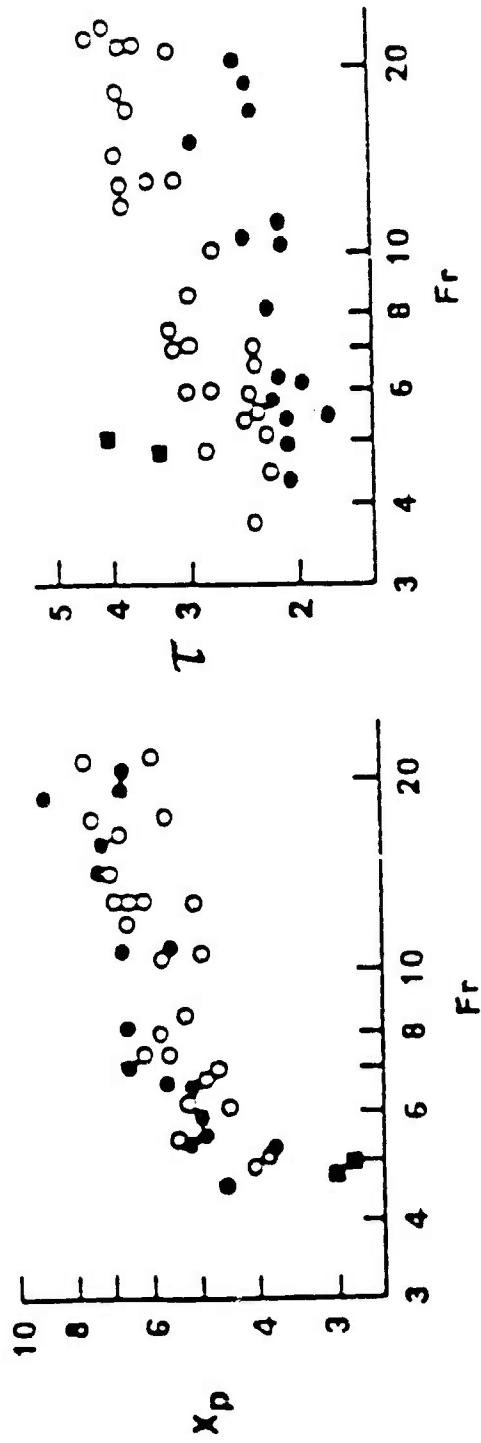


Fig. 14: Non-dimensional opening shock and non-dimensional opening time τ for three C-9 type parachutes, mass ratio 0.13. (Figure taken from Ref. 22)

opening times over the complete Froude number range, and tends to have the greatest opening shock. The 1/4-scale, 0.94 oz/yd², parachute has intermediate values of opening time and opening shock. Obviously, canopy relative stiffness index affects this in some manner, and produces the trends shown.

Based on the above, it was reasoned that the *product* of $X_p\tau$ from Fig. 14 might be suitable as a correlating parameter, where the relative stiffness index determines the value of τ , as in Fig. 8. The product $X_p\tau$, called here "modified impulse," is obviously related to the total deceleration impulse. The total deceleration impulse must be some function of the mass ratio and Froude number, since these quantities are related to the total momentum decrease the payload must experience.

To test this hypothesis, the product of peak opening shock and opening time, $X_p\tau$ (non-dimensionalized), was plotted as a function of Froude number using the data from [9,22]. The results are shown in Fig. 15. Data for both mass ratios of 0.13 and 0.20 are shown on the same figure. The data correlation is seen to be fair and indicates that the hypothesis seems reasonable. However, more work in this area is necessary.

Two points need to be made regarding Fig. 15. First, all the data points from [9,22] are not on this plot because it is sometimes difficult to tell from the [9,22] plots which value of X_p goes with which value of τ when several points are plotted near the same Froude number. However, Fig. 15 contains enough points over a sufficient range of values to define the trend. Second, there is some difference between the values at mass ratio 0.13 and mass ratio 0.20, even though a single curve is faired through the data. This probably reflects the theoretical trend that occurs if Figs. 2 and 3 are combined. Multiplying the data from Figs. 2 and 3 together gives the trends shown on the theoretical plots in Fig. 15. Note that the curve is slightly higher for mass ratio 0.2 than it is for 0.13.

The important fact here is that the experimental trend for $X_p\tau$ vs. Froude number is of the same slope and approximately the same magnitude as predicted by theory.

Use of Modified Impulse Parameter

The manner in which Fig. 15, the modified impulse graph, can be used is as follows. For a given fabric and size of a full-scale or model C-9 parachute, the relative stiffness index, ζ , is calculated using the drop conditions, dimensions and fabric properties. Fig. 8 is used to find the parachute opening time. It should be possible to use this graph to estimate the opening time of other solid flat circular parachutes as well, as long as the design does not deviate too much from the C-9. With the Froude number and mass ratio, Fig. 15 is then used to find the modified impulse. The modified impulse value can then be used to obtain the non-dimensional peak opening shock by dividing the modified impulse by the non-dimensional opening time.

In this manner, the effect of parachute canopy stiffness on both opening time and opening force is taken into account. The graphs apply only for mass ratios in the vicinity of 0.13 to 0.20, however.

Procedures for opening shock for the T-10 canopy and other canopies would be similar to those followed here for the C-9 canopy, except that experimental data over a wide range of model sizes and canopy fabrics would be needed to extend the range for relative stiffness index shown in Fig. 10. Sufficient data on opening force for the T-10 parachute are available from [27] to apply this method over a narrow range of relative stiffness indices for the two canopy fabrics used for this design. However, the time period available for this study did not permit application of the method to the force data for the T-10 parachute.

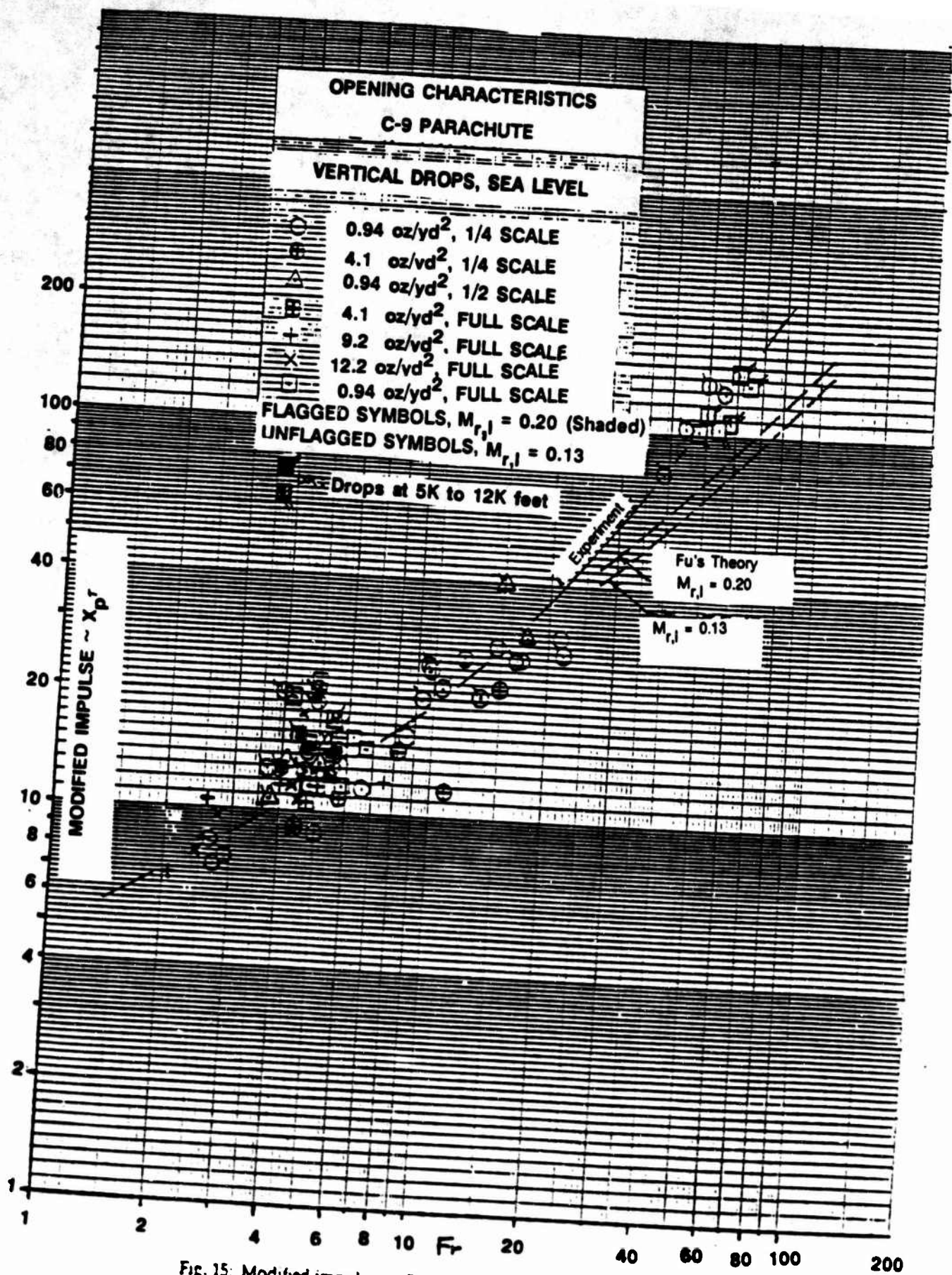


Fig. 15: Modified impulse vs. Froude number for C-9 type parachutes of various configurations and mass ratios.

CLOSURE

Recommendations for Future Research

The current work has brought out a number of areas where further research is needed. Any evaluation of experimental data is somewhat hampered if some simplified theories are not available to guide in interpreting test data. The following quote taken from [30] aptly depicts the situation regarding prediction methods:

The difficulty in predicting the performance of a parachute lies in the complex interaction between the porous canopy and the surrounding flow field. The parachute inflation process involves the unsteady, viscous, compressible flow about a porous body that undergoes large shape changes. Moreover, this body is composed of nonlinear materials with complex strain, strain rate, and hysteresis properties. Thus it is not surprising that a rigorous analysis of the Navier-Stokes equations for the unsteady flow about an inflating parachute presents a formidable challenge to existing computational capabilities. A recent study at Sandia National Laboratories concluded that an axisymmetric flow field solution for a typical weapons parachute would require 3300 hours on a CDC 7600 computer or 330 hours on a CRAY system. Hence, there exists an urgent need for a dependable intermediate theory useful for parachute design.

The theories of Lingard and Fu referenced in the present report seem to provide a reasonable compromise in accuracy without being excessively unwieldy. However, proper verification of these parachute opening theories would require a wide range of tests. The scatter in test data creates this need. Most of these tests would have to be conducted outside the practical range of mass ratios and Froude numbers.

Conversely, at Froude numbers on the order of four to six where opening shock loads are reasonable, extrapolation of Fig. 3 or 4 shows almost no effect of mass ratio on non-dimensional opening force. For this reason further tests need to be conducted at high Froude numbers over a wide range of mass ratios.

Use of Theories to Predict Canopy Stiffness Effects

It would be most valuable to develop a canopy opening dynamics theory that could include simulated canopy stiffness effects in such a way as to confirm the test data trend shown in Fig. 8. It appears that the theory developed by Fu could be used to do this if canopy stiffness effects were simulated by using various input values for

initial semiaperture angle, β_0 (see Fig. 1). Heinrich's stiffness index used the inverted hang test of the canopy and an experimental measurement of D_{\max} to represent canopy stiffness. The D_{\max} and stiffness index values should be reflected in the initial semiapertural angle β_0 in some manner. Fu's theory also allows part of the areal density effect of the fabric to be reflected by making an input change to canopy mass. Some of the effect of canopy stiffness could be accounted for by an adjustment to suspension line elasticity input, but this does not duplicate the main effect of canopy stiffness.

Fu applied his theory only to aircraft drop test data of full-scale 28 ft D_0 C-9 parachutes. The effect of simulated stiffness should be incorporated into the theory and then applied to Lee's drop test data for the 1/2-scale and 1/4-scale C-9 models, and to the full-scale C-9 parachutes that were tested with the heavier fabrics. Some type of correlation between a simulated initial semiaperture angle and a modified hang test of the canopy should be attempted.

Additional Verification of Relative Stiffness Index and Modified Impulse

Only for the C-9 parachute is extensive test data available for various canopy sizes and fabrics. The procedure used to generate the opening time vs. relative stiffness index correlation plot (Fig. 8) should be applied to another parachute type as well. Scale models of the T-10 parachute would be a likely candidate for this since so much full-scale drop data is already available for this parachute. More work also needs to be done to verify the modified impulse correlation concept. The T-10 parachute would be a likely candidate for this study also.

Relative Stiffness for Other Canopy Designs

The relative stiffness index as used in its present form (Eq. (2)) has only been validated for the solid flat circular parachute. It would be desirable to do research to extend this concept to more complicated geometries such as ribbon, ringslot, or cross parachutes.

Conclusion

Theories for parachute opening dynamics, dimensional analyses, and test data have been reviewed to determine the effects of parachute canopy scale and stiffness on the opening characteristics. Based on this work, a new relative stiffness index for parachute canopies has been developed.

It has been shown that this index gives good data correlation for parachute opening times for solid flat circular canopies over a wide range of canopy diameters and fabric areal densities. A modified impulse has been developed based on this stiffness index that gives fair to good correlation for parachute opening shock. The relative stiffness index will make it possible to use scale model wind tunnel and drop test data to predict prototype parachute performance with more confidence than in the past.

Further research needs to be done to adapt the stiffness index to computer programs to simulate the effect of canopy stiffness in the theory. The modified theory then needs to be compared with experiments. Further work also needs to be done to adapt the relative stiffness concept to other types of parachute canopies.

REFERENCES

1. Kaplun, S., "Dimensional Analysis of the Inflation Process of Parachute Canopies," Aeronautical Engineer Thesis, California Institute of Technology, Pasadena, California, 1951.
2. Barton, R.L., "Scale Factors for Parachute Opening," NASA TN-D-4123, Manned Spacecraft Center, Houston, Texas, September 1967.
3. French, K.E., "Model Law for Parachute Opening Shock," *AIAA Journal*, Vol. 2, No. 12, p. 2226-2228.
4. French, K.E., "Dimensionless Products of Parachute Inflation," *Journal of Spacecraft and Rockets*, Vol. 6, No. 10, October 1969, pp. 1199-1200.
5. Fu, K-H., "Theoretical Study of the Filling Process of a Flexible Parachute Payload System," German Air and Space Research and Test Institute, Braunschweig, Germany, 1975.
6. Lingard, J.S., "The Aerodynamics of Parachutes During the Inflation Process," Ph.D. Thesis, Department of Aeronautical Engineering, University of Bristol, England, October 1978.
7. Heinrich, H.G., and Hektner, T.R., "Flexibility as a Model Parachute Performance Parameter," *Journal of Aircraft*, Vol. 8, No. 5, September 1971, p. 704.
8. Ewing, E.G., Bixby, H.W., and Knacke, T.W., "Recovery Systems Design Guide," AFFDL-TR-78-151, December 1978.
9. Lee, C.K., "Experimental Investigation of Full-Scale and Model Parachute Opening," Proceedings of the AIAA 8th Aerodynamic Decelerator and Balloon Technology Conference, New York, 1984, pp. 215-223.
10. Steeves, E., "Dimensional Analysis of the Airdrop Problem," private communication, U.S. Army Natick Research, Development and Engineering Center, Natick, Massachusetts, 1983.
11. Mueller, W., "Parachutes for Aircraft," *Zeitschrift fuer Flugtechnik und Motorluft-schiffahrt*, Heft No. 20, 1927.
12. Weinig, F.S., "On the Dynamics of the Opening Shock of a Parachute," USAF Office of Aeronautical Research, WADC, Dayton, Ohio, TR-6, February 1951.
13. Roberts, B.W., "Aerodynamic Inflation of Shell Type Parachute Structures," *Journal of Aircraft*, Vol. 11, July 1974, pp. 390-397.

14. Payne, P.R., "A New Look at Parachute Opening Dynamics," *Aeronautical Journal*, Vol. 11, February 1973, pp. 85-93.
15. Wolf, D.F., "A Simplified Dynamic Model of Parachute Inflation," *Journal of Aircraft*, Vol. 11, January 1974, pp. 28-33.
16. McVey, D.F., and Wolf, D.F., "Analysis of Deployment and Inflation of Large Ribbon Parachutes," *Journal of Aircraft*, Vol. 11, February 1974, pp. 96-103.
17. O'Hara, F., "Notes on the Opening Behaviour and the Opening Forces of Parachutes," *Royal Aeronautical Society Journal*, Nov. 1949, pp. 1053-1062.
18. Heinrich, H.G., and Bhateley, I.C., "A Simplified Analytical Method to Calculate Parachute Opening Time and Opening Shock," Summer Course on Aerodynamic Deceleration, University of Minnesota, July 1961.
19. Heinrich, H.G., "A Linearized Theory of Parachute Opening Dynamics," *Royal Aeronautical Society Journal*, Vol. 76, December 1972, pp. 723-730.
20. Heinrich, H.G., and Saari, D.P., "Parachute Opening Shock Calculations with Experimentally Established Input Functions," *Journal of Aircraft*, Vol. 15, No. 2, February 1978, pp. 100-105.
21. Calligeros, J.M., and Dugundji, J., "Similarity Laws for Aerothermoelastic Testing," *Journal of the Aerospace Sciences*, Vol. 29, No. 8, August 1962, pp. 935-950.
22. Lee, C.K., "Modeling of Parachute Opening: An Experimental Investigation," *Journal of Aircraft*, Vol. 26, No. 5, May 1989, pp. 444-451.
23. Steeves, E.C., "A Linear Analysis of the Deformation of Pressure Stabilized Beams," U.S. Army Natick Laboratories TR-75-47-AMEL, Natick, Massachusetts, January 1975.
24. Remington, P.J., O'Callahan, J.C., and Madden, R., "Analysis of Stresses and Deflections in Frame Supported Tents," U.S. Army Natick Laboratories TR-75-31, Natick, Massachusetts, April 1974.
25. Render, A.B., and Bradley, P.D., "The Development of a Parachute Strain Measurement Technique," Proceedings of the AIAA 9th Aerodynamic Decelerator and Balloon Technology Conference, Albuquerque, New Mexico, October 1986, pp. 194-202.
26. Monego, C.J., and Pilsworth, M.N., Jr., "Development of an Apparatus for Biaxial and Shear Stress-Strain Testing of Fabrics and Films," Natick TR-80/028, 1980.

27. Watson, L.L., "Opening Parameters of 35 ft D₀ Extended Skirt Parachute," AIAA Paper No. 75-1367, AIAA, New York, 1975.
28. Heinrich, H.G., and Hektner, T.R., "Opening Dynamics of a T-10 Parachute with Inflation Aids," AFFDL-TR-69-112, Wright Patterson AFB, Ohio, March 1970.
29. Goodrick, T.F., "A Quick Look at Reduction of Opening Shock Using a Damped Spring," Technical Memo, U.S. Army Natick Research, Development and Engineering Center, Natick, Massachusetts.
30. Muramoto, K.K., and Garrard, W.L., "A Method for Calculating the Pressure Field about a Ribbon Parachute Canopy in Steady Descent," Proceedings of the 8th Aerodynamic Decelerator and Balloon Technology Conference, Hyannis, Massachusetts, April 1984, pp. 57-67.